RESEARCH TRIANGLE INSTITUTE

RTI/5123/91-92 Quarterly March 1992

LARGE-AREA, PLASMA-ASSISTED, HALOGEN-BASED DIAMOND DEPOSITION

Quarterly Report - First and Second Quarters

R.A. Rudder
R.J. Markunas
M.J. Mantini
G.C. Hudson

Office of Naval Research
Program No.
N00014-91-C-0177

POST OFFICE BOX 12194 RESEARCH TRIANGLE PARK, NORTH CAROLINA 27709-2194

REPORT DOCUMENT PAGE

Form Approved
OMB No 0704-0188

1. AGENCY USE ONLY *(Leave blank)*	2. REPORT DATE	3. REPORT TYPE AND DATES COVERED
	March 4, 1992	Combined 1st and 2nd quarterly report covering the period 9/391 to 12/3/91 and the period 12/3/91 to 3/3/91

4. TITLE AND SUBTITLE

Large Area Plasma-Assisted, Halogen-Based Diamond Deposition

5. FUNDING NUMBERS

N-00014-91-C-0177

6. AUTHOR(S)

R. A. Rudder

7. PERFORMING ORGANIZATION NAME(S) AND ADDRESS(ES)

Research Triangle Institute
P. O. Box 12194
Research Triangle Park, NC 27709

8. PERFORMING ORGANIZATION REPORT NUMBER

83U-5123

9. SPONSORING/MONITORING AGENCY NAME(S) AND ADDRESSES(ES)

Office of Naval Research
800 N. Quincy Street
Arlington, VA 22217-5000

10. SPONSORING/MONITORING AGENCY REPORT NUMBER

11. SUPPLEMENTARY NOTES

12a. DISTRIBUTION/AVAILABILITY STATEMENT

Approved for public release; unlimited distribution

12b. DISTRIBUTION CODE

13. ABSTRACT

A number of chemical systems have been evaluated for diamond growth in the parallel plate capacitive systems. Unlike previous work in the rf inductive systems, diamond growth from H_2/CH_4, H_2/CH_1, and H_2O/CH_3OH systems in the parallel plate was not forthcoming. Analysis of the critical differences between the rf inductive vs rf capacitive coupling identified the plasma density and the degree of plasma dissociation to be the substantial differences. We have embarked on a course to evaluate scale of the rf inductive technology by development of a planar inductive coil which would merely replace the capacitive plate on standard large area rf system. Preliminary results show that creation of a high density plasma at low pressures and modest power levels over a 100 nm area is feasible with the current 500W power supply. No diamond growths have yet been attempted.

14. SUBJECT TERMS

15. NUMBER OF PAGES

16. PRICE CODE

17. SECURITY CLASSIFICATION OF REPORT	18. SECURITY CLASSIFICATION OF THIS PAGE	19. SECURITY CLASSIFICATION OF ABSTRACT	20. LIMITATION OF ABSTRACT
UNCLASSIFIED	UNCLASSIFIED	UNCLASSIFIED	

LARGE-AREA, PLASMA-ASSISTED, HALOGEN-BASED DIAMOND DEPOSITION

ARPA NO: NA
Contract No: N00014-91-C-0177

Client: Office Of Naval Research
Source: Office Of Naval Research
Contract Amount: $197,769

Effective Date of Contract: 09/03/91
Expiration Date of Contract: 07/14/92

Principal Investigator: R.A. Rudder
Telephone No.: (919) 541-6765

Reporting Period: Combined Quarterly Report Covering the Periods 9/03/91 to 12/03/91 and the Period 12/03/91 to 3/03/92

Fiscal Status:

Total:	$ 197,769
Expended:	153,752
Remaining:	44,017

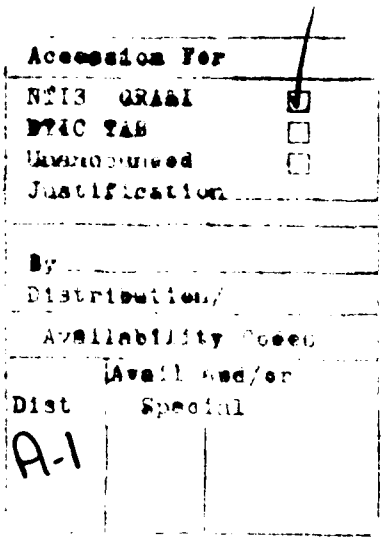

TABLE OF CONTENTS

1.0 INTRODUCTION

This is a combined quarterly report on contract N00014-91-C-0177 covering the period Sept. 03, 1991 to Dec. 03, 1991 and the period Dec. 03, 1991 to March 03, 1992.

The large area diamond program at Research Triangle Institute began last September focusing on transferring to the rf parallel plate the diamond growth technologies (i e. the chemical systems requiring low power densities) that we had so successfully used for diamond growth in a 13.56 MHz inductive growth system. The impetus for such a transfer was to develop a large area technology for diamond growth which could immediately impact industrial manufacturing by giving economy of scale to the diamond growth process.

Prior to beginning the program, Research Triangle Institute developed an exciting new technology for diamond growth in the inductive system which seemingly should have a large impact on diamond manufacturing costs. Using first vapors from water:alcohol and later using water:acetic-acid:alcohol solutions, we demonstrated the growth of diamond polycrystalline and homoepitaxial films. No explosive compressed gasses were used in these processes. Vapors from the solutions leaked into low pressure (0.5 - 1.0 Torr) rf discharges. Diamond production occurred at far lower powers and temperatures than we had heretofore been able to use from traditional hydrogen based processes. Given the lower required plasma powers, the lower growth temperatures, the absence of explosive or compressed gasses, and the low pressures, the water-based process is ideally suited for large area diamond deposition.

Beginning the program, we installed hydrogen gas on the parallel plate reactor with CH_4 and CF_4 gasses available through a gas manifold. Neither the H_2/CH_4 system nor the H_2/CF_4 system readily yielded diamond growth. The H_2/CH_4 system never produced significant growth. Growths were typically 10-12 hours in duration. The H_2/CF_4 system suffered from Al contamination. In conjunction with our work at RTI,

Richard Koba at Plasma Therm also attempted diamond growth from halogen based systems. While we were not privileged to all information concerning their experimental detail, it seemed appropriate to divide the work of the program so as to let Plasma Therm investigate extensively the halogen-based work while we concentrated more on the water-based systems. Given the high powers that we had been using in the rf inductive systems for all the hydrogen-based processes, it seemed reasonable that we were not achieving a high enough power density in the parallel plate system. (At this time, power density seemed to be a useful comparator.) The water-based systems from our experience with the rf inductive discharges were requiring lower input powers as compared to what we had used for either the H_2/CH_4 of the H_2/CF_4. Correspondingly, we made attempts to deposit diamond in the parallel plate system using H_2O/CH_3OH and $H_2O/CH_3COOH/CH_3OH$. These early attempts did not deposit diamond. Analysis of the experiments (included here) have provided critical insight into the rf-plasma environment necessary for diamond growth.

We began to analyze the critical differences between the capacitive and inductively coupled rf systems. Optical emission spectroscopy and mass quadrupole spectroscopy were used to assess the critical differences between the capacitive and the inductive systems. We made great strides in understanding the fundamental differences, and we now see avenues by which we can expand the low pressure rf technology for large area diamond deposition. This report details the critical differences between the capacitive and inductive systems and shows progress towards planar inductive technology.

Prime outputs from the phase of the program are:

1) critical analysis of the differences between rf capacitance and rf inductive coupling using optical emission and quadrupole mass spectroscopy.

2) identification of differences between rf capacitive and rf inductive coupling from literature reports showing a two-order magnitude increase in plasma density between capacitive and inductive coupling.
3) preliminary design and testing of re-entrant rf coils of which a planar inductive coil could easily replace a planar capacitive plate on standard plasma-assisted chemical vapor deposition systems.

These results now position us in the last phase of this program to concentrate on large area diamond growth using scaled-up induction coils. Critical to this development has been a demonstration here at RTI of a re-entrant induction coil that resides in the vacuum vessel. Such a design will have the best power coupling to the plasma gas. Consequently allowing larger area growth with lower power input.

2.0 COMPARISON OF THE CAPACITIVE AND INDUCTIVE COUPLING

2.1 Optical Emission Spectroscopy

The simplest plasma characterization to perform is optical emission spectroscopy. Besides optical emission, we have performed quadrupole mass spectroscopy on gasses pumped from water-alcohol discharges. The water-methanol system has been studied as a function of alcohol concentration in the water mixture for both inductive and capacitive couplings. Analysis on the water-methanol system for the inductively-coupled configuration reveals a number of fascinating findings. We are reporting on those studies for the inductive coupling both at the International Society for Hybrid Microelectronics Diamond Workshop March 30 - April 1 and at the International Conference on Metallurgical Coatings and Thin Films April 6 -10. A copy of the preprint submitted to the ICMCTF is enclosed in the appendix.

We have chosen the water-alcohol based system for comparison between the capacitive and inductive cases. The water-alcohol system offers one the opportunity to discern parent molecules introduced into the discharge from reaction products created by the discharge. Atomic hydrogen emission dominates the emission spectrum from rf inductive discharges of both water and molecular hydrogen. Figures 1 and 2 show optical emission data from diamond producing inductive discharges containing 1% CH_4 in H_2 and 50% methanol in H_2O. The emission at 656 nm (highlighted by an arrow in each figure) is from the n=3 to n=2 transition. The n=3 transition is ~ 12 eV above the hydrogen ground state. Intense emission from this transition is thus indicative of a dense energetic electron population. In contrast, optical emission from capacitively coupled water discharges show primarily OH emission lines. Figure 3 shows emission from a capacitively coupled water discharge. One observes only a small amount of atomic hydrogen emission from the capacitively coupled water discharges. Primarily, the

emission is from OH species. One explanation for this difference may be that the degree of dissociation in capacitively-coupled discharges is not as high as the degree of dissociation occurring in the inductively-coupled discharges. As a consequence, the atomic hydrogen population is not as substantial in the capacitively coupled system. Indeed, we shall see from mass quadrupole data that neither the water nor the methanol is as completely dissociated in the capacitively coupled systems as they are in the inductively coupled system. It also may be true that the electron population in the capacitively coupled plasmas has to low an energy to excite the atomic H transitions at the n=3 (12 eV) level above ground.

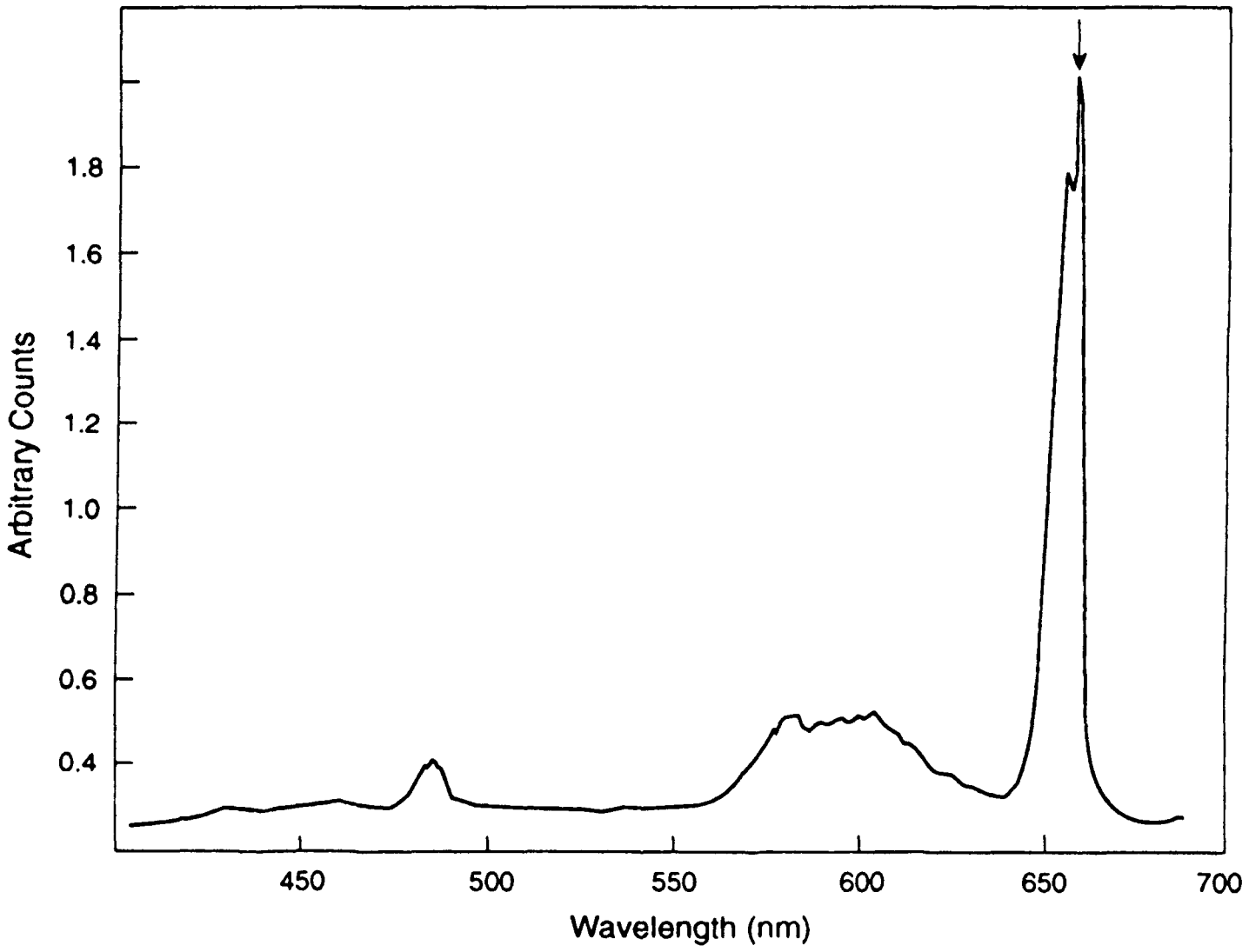

Figure 1. Optical emission spectrum from a high power, inductively coupled, 1% CH_4 in H_2 diamond producing discharge at 3 Torr.

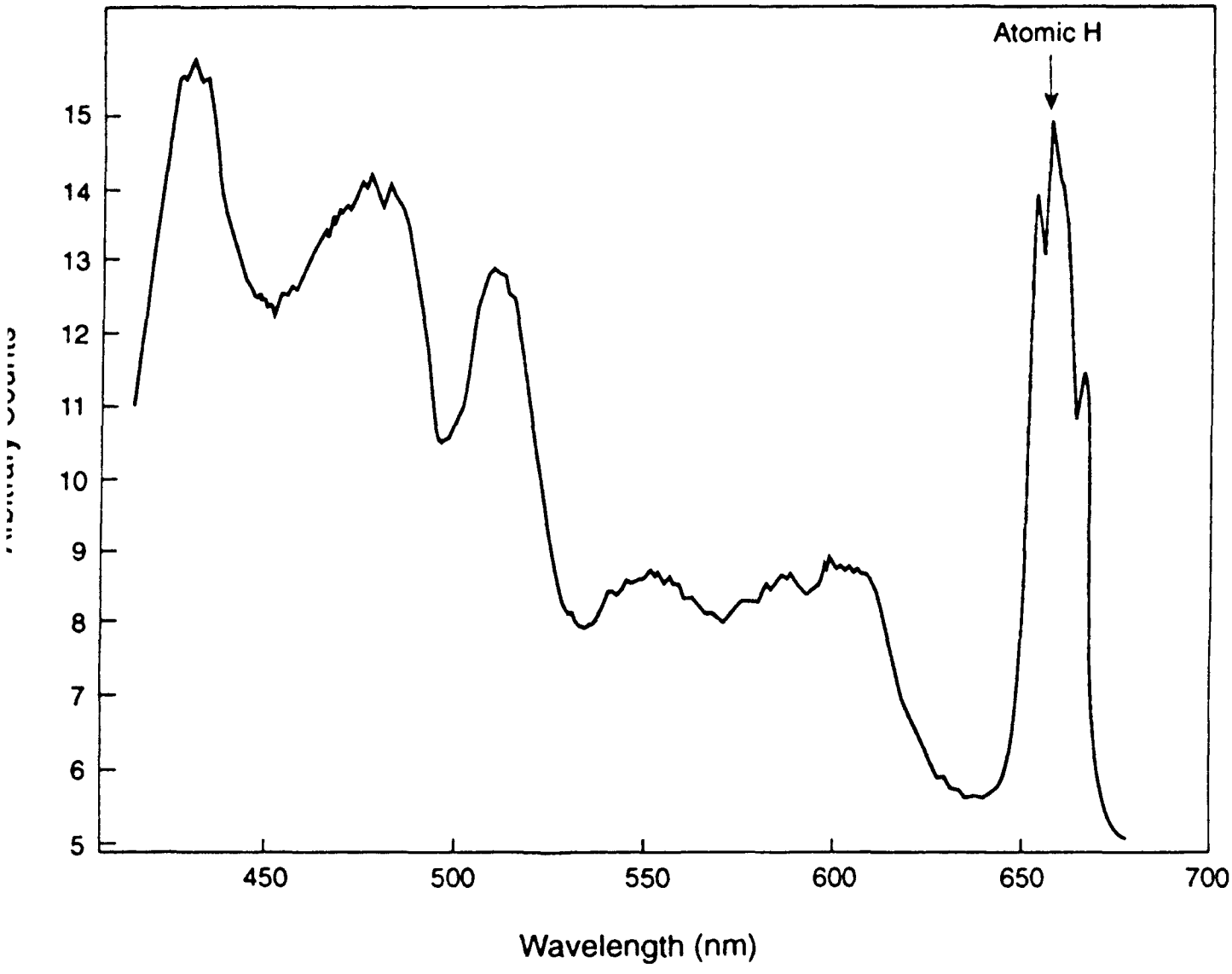

Figure 2. Optical emission spectrum from a low power, inductively coupled, 50% CH_3OH in H_2O diamond producing discharge at 1.0 Torr.

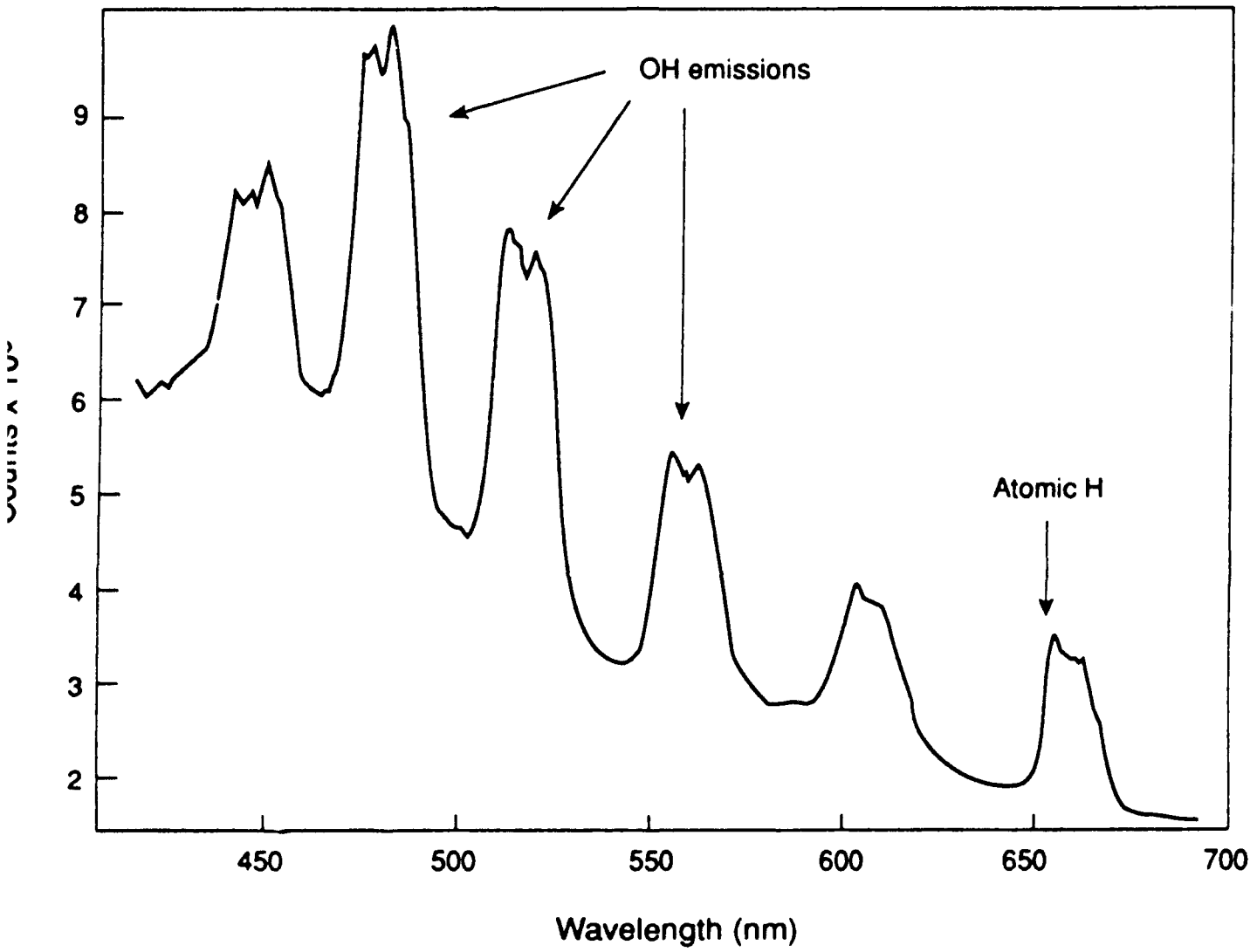

Figure 3. Optical emission spectrum from a capacitively coupled water discharge at 1.0 Torr.

2.2 Quadrupole Mass Spectroscopy

In addition to optical emission, quadrupole mass spectroscopy has been used to assess differences in capacitive and inductive coupling. Figure 4 shows H_2O^+ and CH_3O^+ ion counts before and after initiation of an inductive water:methanol plasma. Figure 4 also shows those ion counts as a function of the volumetric concentration of methanol in the liquid reservoir. Before initiation of the plasma, the ratio of H_2O^+ and CH_3O^+ ion counts reflect Raoult's Law relating the partial pressures above a liquid reservoir to the vapor pressure of each constituent times the mole fraction of that constituent in solution. However, after plasma initiation, a rather dramatic occurrence is observed. Nearly all the CH_3OH is converted upon traversing the plasma. (Note that the mass quadrupole samples gasses after they have traversed the plasma tube.) The CH_3O^+ counts after plasma initiation is only a couple percent of the original CH_3O^+ counts. Even more knowledge of the plasma dissociation is obtained when one examines by-products from the H_2O:CH_3OH plasma discharge. Figure 5 shows the dominant conversion products observed as a function of methanol concentration in the reservoir. A high fraction of hydrogen is produced in the gas phase almost regardless of the CH_3OH concentration. Notice that the hydrogen production is approximately constant regardless of methanol concentration. This is to be expected if both the water and methanol are both being equally dissociated. Both H_2O and CH_3OH have the same atomic fraction of H. Molecular H_2 is the dominant species produced by the H_2O:CH_3OH plasma discharge. CO and C_2H_2 are also produced as a by-product of the H_2O:CH_3OH plasma discharge. At high water concentrations (i.e. high O fraction), CO is the preferred gaseous carbon product. At high CH_3OH concentrations (i.e. low O fraction), C_2H_2 is the preferred gaseous carbon product. Thus, we have identified H_2, CO, and C_2H_2 as conversion products in the high density water-methanol plasma discharges. The water concentration in the discharges remains high (20-30%), but the CH_3OH concentrations

are reduced to only a small percentage of their original concentrations. The plasma production of CO and C_2H_2 could have occurred via direct conversion of CH_3OH into CO or C_2H_2. Alternatively, gasification of solid carbon through interactions of O and H with graphite could also contribute to the CO and C_2H_2 counts.

It is abundantly clear that the water-based processes convert parent H_2O and CH_3OH molecules into more stable high temperature products. One might define an effective temperature of the plasma by comparing the H_2O to H_2 conversion in the plasma to that predicted from thermodynamic equilibrium theory for water dissociation at high temperatures. Lede et. al. have reported on the direct thermal decomposition of water at elevated temperatures (1500-4000 K) at pressures from 10^4 to 10^6 Pa. [Figure 6 is a photocopy of Lede's data at 10^4 Pa.] At temperatures in excess of 3300 K, H_2O is no longer the dominant species. Atomic H and atomic O are the dominant species at high temperature. From the quadrupole data in Figure 5, one can estimate the partial pressure of H_2O in the system when only water vapor is admitted to the discharge. By taking into account differences in ionization efficiency and differences in mass conductances of H_2, H_2O, and CO, we estimated the partial pressure of H_2O in the growth chamber with the discharge on to be 0.28 Torr. Compared to the partial pressure of 1 Torr for H_2O in the system before the discharge was initiated, the amount of H_2O dissociated by the plasma is 72%. Referring to the thermodynamic equilibrium data given by Lede et. al. [21], dissociation of 72% of the water would require a temperature of ~ 3100 K for homogeneous dissociation. In prior work using H_2:CH_4 discharges, we calculated an effective temperature based on a Boltzman distribution to the atomic hydrogen population. Those calculations also predicted temperature around 3000 K. Thus, the low pressure rf induction technique generates an extremely hot plasma. One key to the success of the growth of diamond at low pressures is undoubtedly the high generation rate of atomic hydrogen in these rf induction discharges. At low pressures, atomic H can rapidly diffuse from the plasma discharge and recombine on reactor walls. The diffusion

depletes the gas phase of atomic H. Correspondingly, high generation rates must occur in order to maintain a high concentration of atomic hydrogen in the plasma. The high generation rates are insured by the high temperatures of the rf induction plasma.

We have analyzed quadrupole data from the water-based capacitively coupled discharges. This work indicates that molecular H_2 and the other conversion products are not as prevalent in the capacitively coupled systems. Figures 7 and 8 show the parent and conversion products for the water-methanol capacitively coupled system as a function of methanol concentration in the liquid reservoir. While the same by-products are observed in the capacitively coupled system as in the inductively coupled system, there are a number of important differences:

- the molecular hydrogen production (i e. the water dissociation) is not as nearly complete in the capacitively coupled system.
- the dependence of CO production is remarkably difference between the two systems.

The dependence of CO production on CH_3OH concentration in Figure 7 (conversion products for the capacitive system) is different from the dependence of CO production on CH_3OH concentration in Figure 5 (conversion products for the inductive system). The CO dependence increases with CH_3OH in the capacitive system while it decreases with CH_3OH concentration in the inductive system. If the origin of CO is CH_3OH partial dissociation, then CO production should increase along with the CH_3OH concentration. Indeed that is what we observe in Figure 7 for the capacitive coupling. If, however, the plasma is atomizing the H_2O and CH_3OH molecules, then the reduced O content at higher CH_3OH concentrations should result in lower CO concentrations. In both figure 5 and 7, we have noted the relative oxygen concentrations for pure water and pure methanol. One can see that the CO production correlated with the overall oxygen content for the inductively coupled discharge.

This data, like the optical emission, confirms that the capacitively coupled

discharges are not as dissociative as the inductively coupled discharges are. This data shows quite eloquently how it situ sensing can be used to ascertain critical processing information. Indeed effective temperatures and dissociations can be routinely verified during diamond growth. If desired, the conversion from H_2O:CH_3OH to H_2:CO:C_2H_2 can be used in an artificially intelligent growth model which is controlling the diamond film growth.

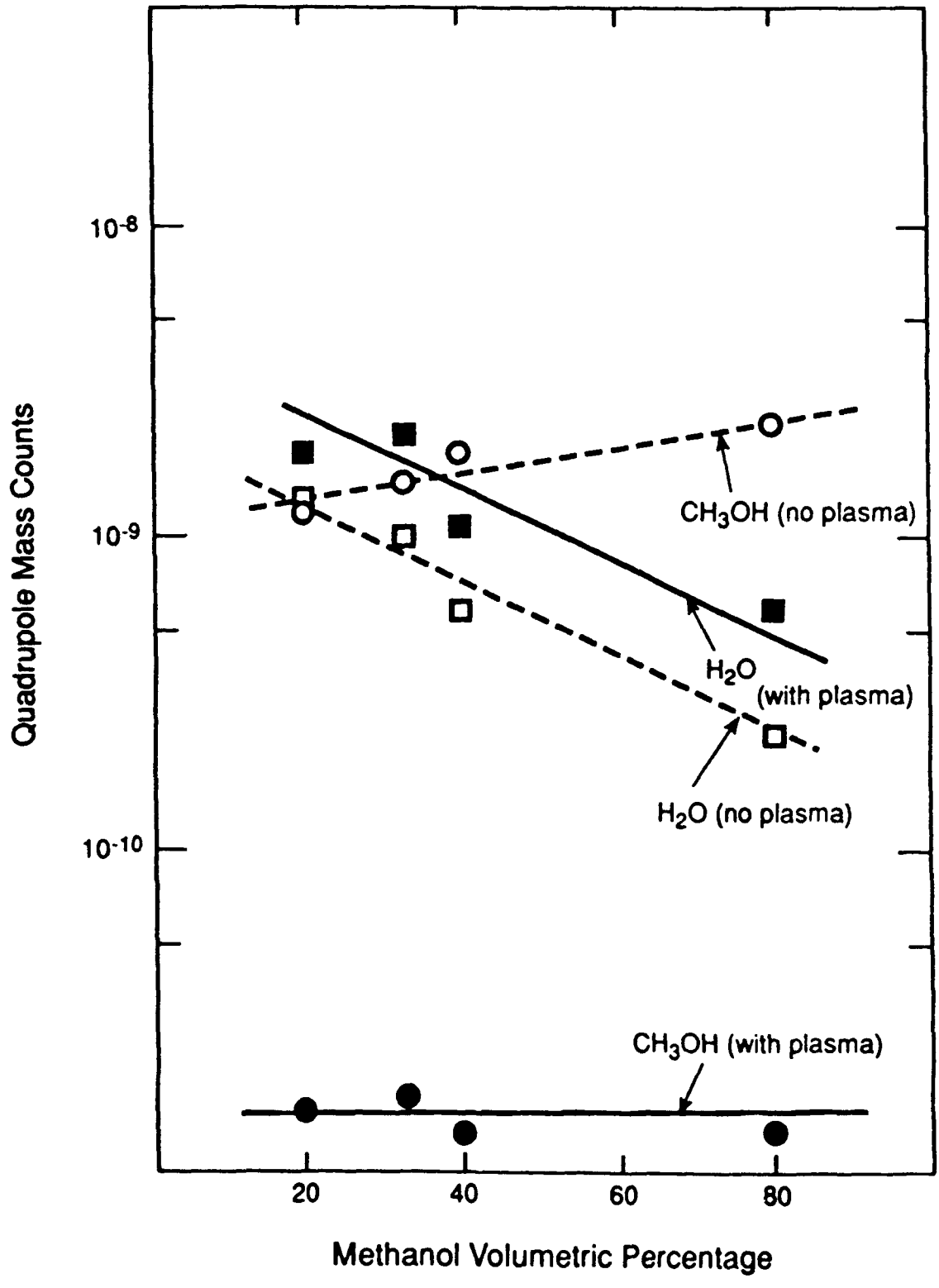

Figure 4. Parent products before and after initiation of an inductively coupled H_2O:CH_3OH discharge as a function of CH_3OH concentration in the liquid reservoir.

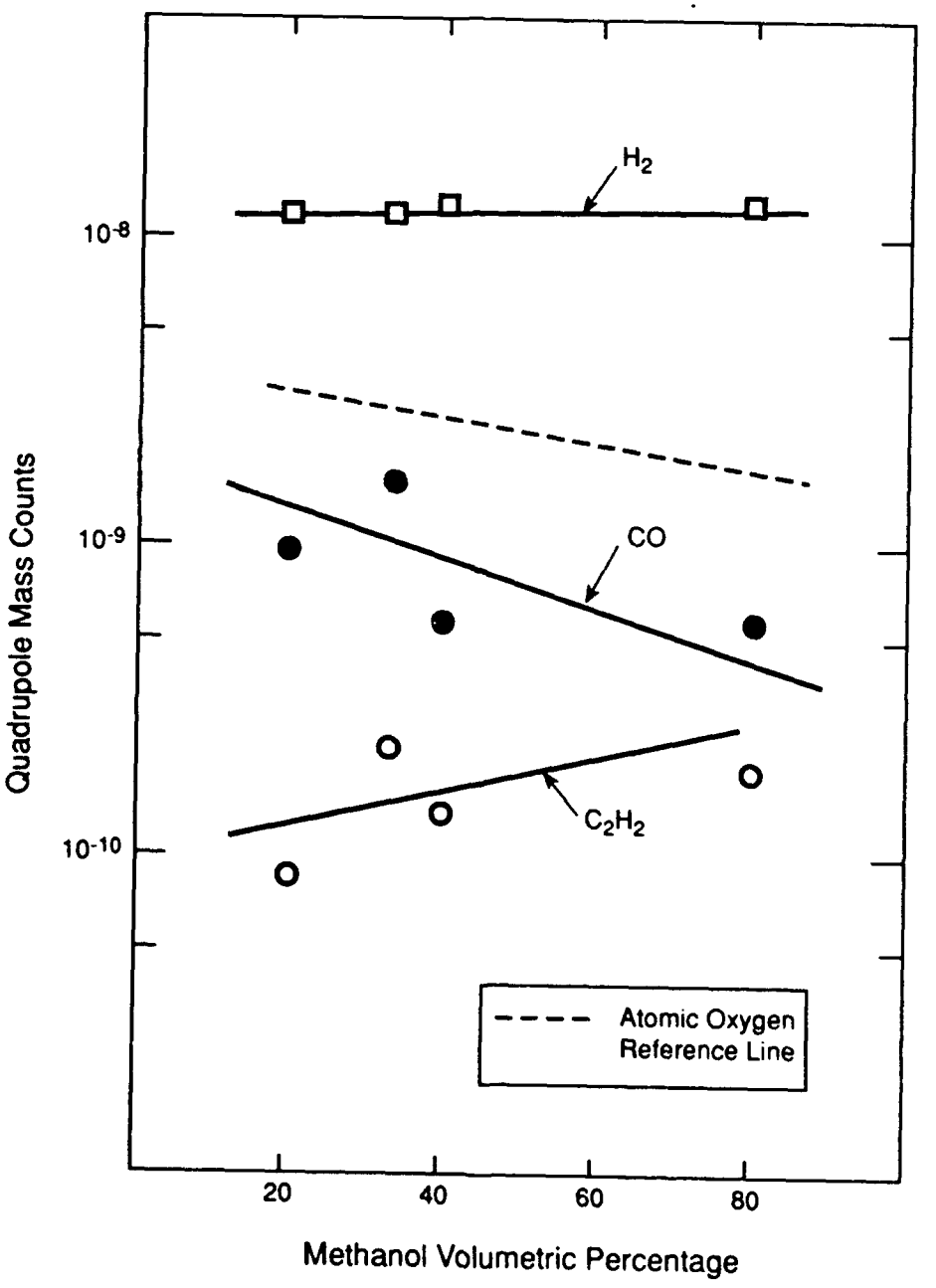

Figure 5. Conversion products observed on inductively coupled H_2O:CH_3OH discharge as a function of CH_3OH concentration in the liquid reservoir.

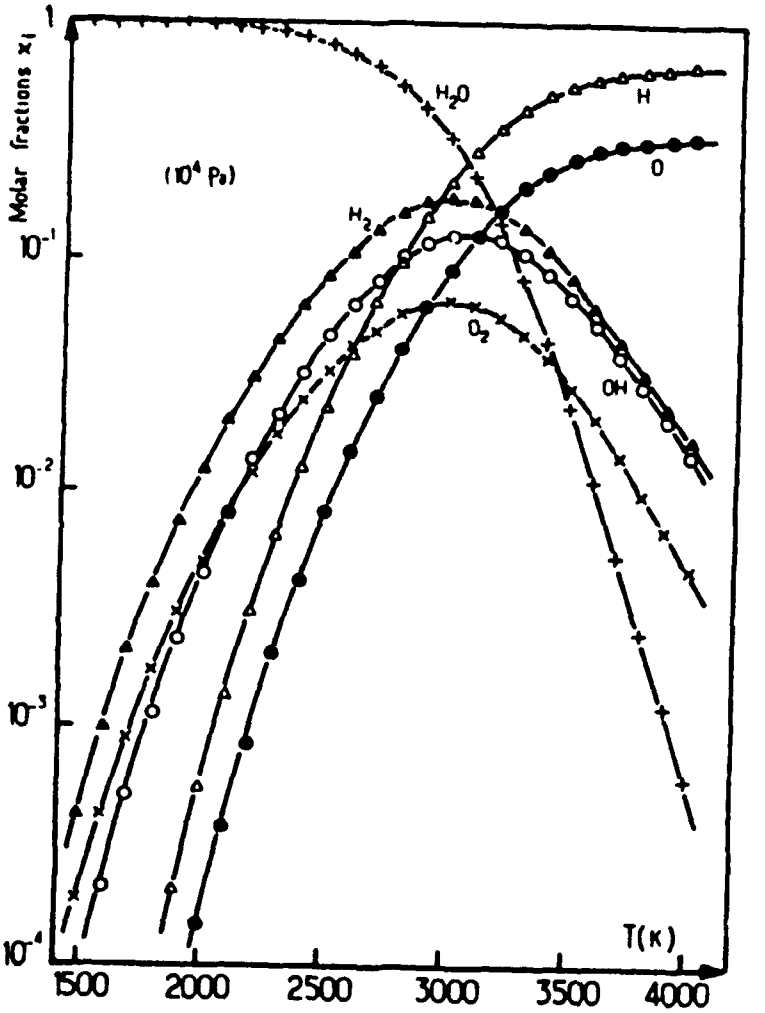

Figure 6. Thermal dissociation of water at 10^4 Pa (courtesy of Lede et al. Int. J. of Hydrogen Energy, 7, 939 (9182)).

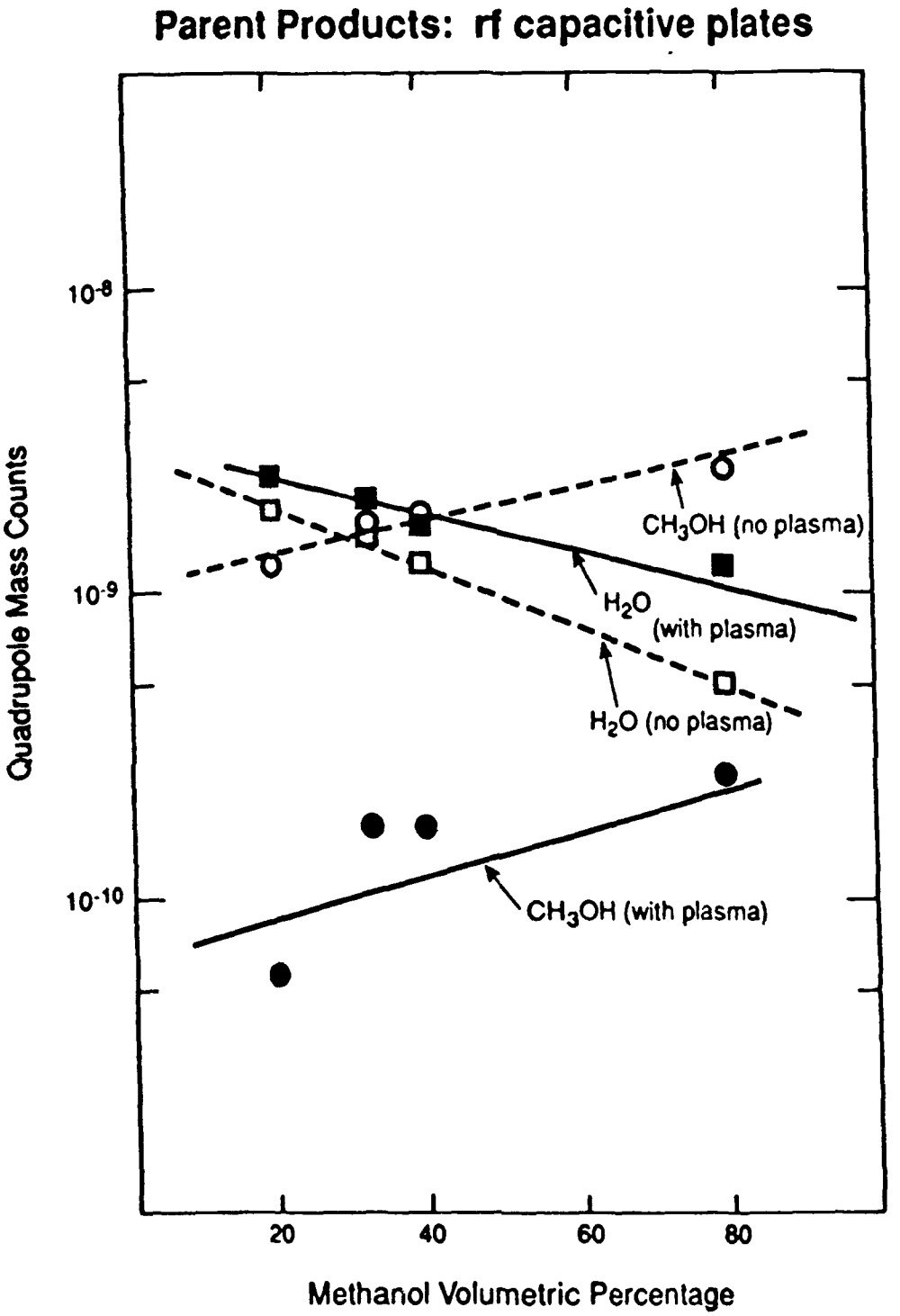

Figure 7. Parent products before and after initiation of a capacitively coupled H_2O:CH_3OH discharge as a function of CH_3OH concentration in the liquid reservoir.

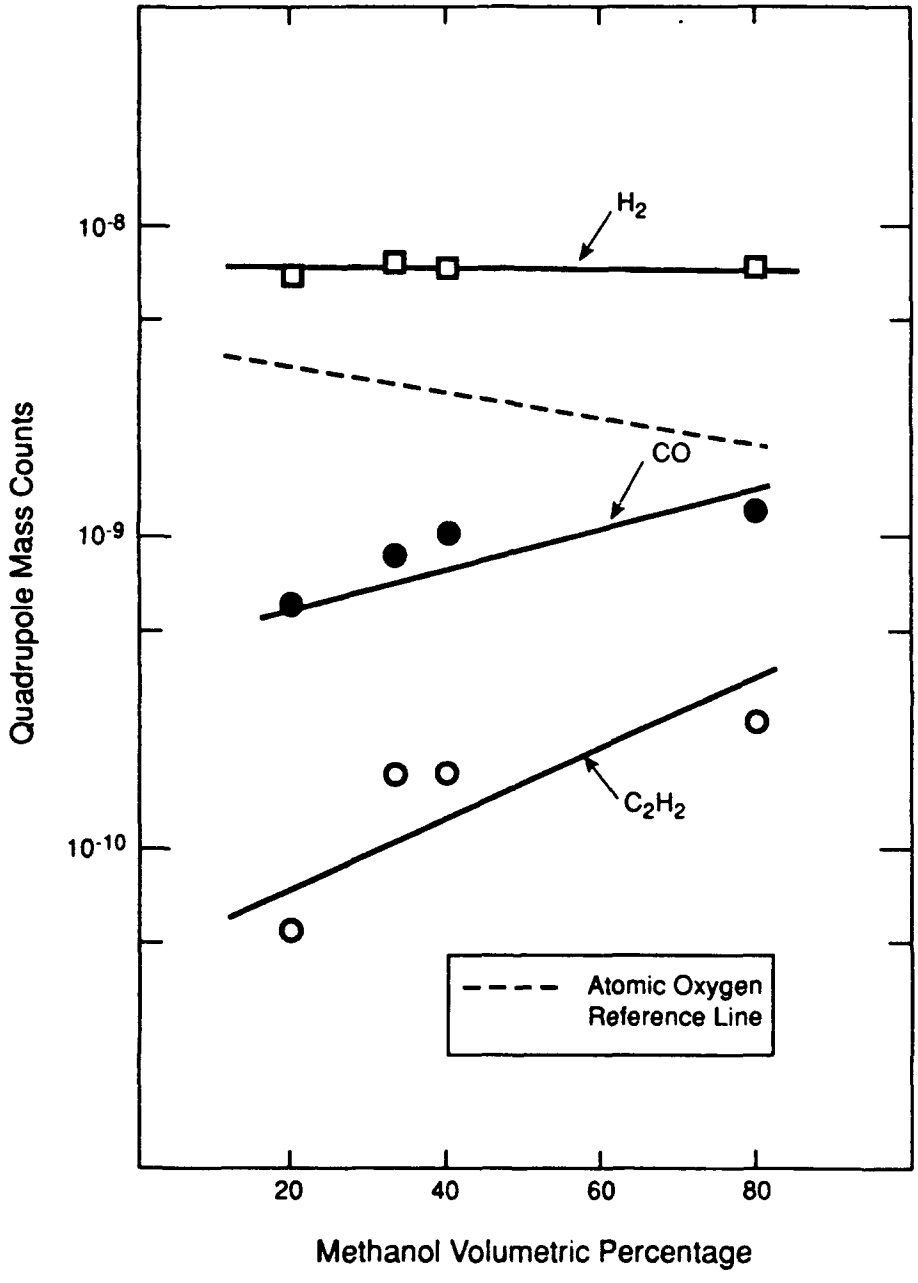

Figure 8. Conversion products observed in a capacitively coupled H_2O:CH_3OH discharge as a function of CH_3OH concentration in the liquid reservoir.

3.0 PLASMA COUPLING

Recognizing different phenomenological behavior for diamond growth from induction in capacitive systems, we began to address the issue of inductive vs. capacitively coupled plasmas. Fortunately, the "Proceedings of the Workshop on High-Density Plasma Techniques and Processes for Integrated Circuit Fabrication" was recently published in the Journal of Vacuum Science and Technology B, vol. 9 March/April 1991. In that Proceedings, J. Amorim et al. reported on "High-density-plasma made of an inductively coupled radio frequency discharge", pp 362-365. Those workers clearly established using Langmuir probes that rf inductively coupled discharges can produce extremely high density plasmas. Figure 9 is taken from the work of J. Amorim et. al. Plasma densities of 5 x 10^{12} cm^3 were achieved with only 300-400 W of applied power to 0.10 Torr Ar discharge. Those workers showed that (at lower power) the discharge is essentially sustained through capacitive coupling to the voltage on the rf coil. This capacitive coupling produces a very diffuse plasma with a density of only 2 x 10^{10} cm^3. As shown in Figure 9, the transition from capacitive coupling to induction coupling occurs as a very abrupt transition. For example at 130 mTorr, an increase in power from 250 to 275 W increases the electron density by two orders of magnitude. As a consequence, it can be deduced that inductive coupling, while occurring at somewhat a higher power level, is far more efficient in coupling power to the plasma gas than capacitive coupling. Higher plasma densities ultimately translate into higher deposition rates. Achieving induction coupling and, thus, a high plasma density efficiently translates into better power utilization and correspondingly lower manufacturing costs.

It, thus, seems likely that the failure to observe diamond growth with the capacitively coupled parallel plate is a consequence of the two-order of magnitude reduction in plasma density. This results in the poor plasma dissociation and lower chemical reactivity. If the two-order of magnitude reduction in plasma density

compromised the growth rate by the same factor, then the 10 hr depositions would in the parallel plate system have only produced 5 nm of diamond growth. Assuming non-uniform nucleation, we would conclude (as we did) that no diamond growth had occurred.

Critical to the diamond growth in all the rf inductive processes is the establishment of a high density plasma. While the amount of power necessary to achieve a high density plasma varies from one gas mixture to another, in general, lower pressure discharges require less power to achieve induction coupling. Figure 10 is a plot of the critical power necessary to achieve a high density plasma for the H_2:CH_4 and H_2O:CH_3OH systems as a function of pressure. The threshold power necessary to establish the high density plasma varies almost linearly with pressure (in this pressure range) for the H_2O:CH_3OH system. The H_2:CH_4 system behaves supralinearly so that at higher pressures there is a significant power difference between operating a water-based process verses a molecular-hydrogen-based process.

What fundamentally is the reason for poor plasma coupling in capacitive systems?

Perhaps, the simplest way to consider the differences between rf capacitive and rf inductive coupling (perhaps to simplistic) is to consider the plasma a conducting media in which we want to generate the maximum current flow per input power. In rf capacitive-coupling because of differences in electron and ion mobility, a capacitive sheath develops near the powered electrode and at the grounded electrode. Consequently, a complex impedance (Z) exists between the powered electrode and ground. Resonance conditions can be determined for this complex impedance, but (typically at standard pressures and frequency of operation) one is not operating in resonance. Current flow in the plasma is determined by diffusion to the plasma sheaths where ions are accelerated across the sheaths. The ions, upon impact with the cathode, cause secondary electron emission. The electrons are accelerated across the sheath into the plasma. Those accelerated

secondary electrons are responsible for sustaining the plasma. Herein lies the fundamental problem. Electrons in the plasma are shielded from the primary electric fields. Sustaining a capacitively coupled plasma requires creation of secondary electron emission via ion impact on the cathode. The vast majority of energy is dissipated as heat on the cathode. (It is perhaps informative to remember that dc arc discharges which have a capacitive arrangement only sustain the arc when the cathode becomes a hot thermal emitter.)

Inductive-coupling on the other hand relies only on the electromotive force (EMF) developed by the changing magnetic flux. Current oscillation in the inductor produces a changing magnetic flux density proportional to the current, $I \sin(\omega t)$. The EMF is then proportional to ωI. At high frequencies and with high circulating currents in the coil (high Q in the external matching circuit), the EMF will establish induction currents in the plasma similar to currents induced in conducting metals subjected to the same EMF. The induction currents are circuitous within the plasma gas and do not depend on an electron supply from a cathode. The penetration of magnetic force lines into the plasma allows electrons in the body of the plasma to experience EMF and gain energy. Electromotive forces supply energy to the plasma gas necessary to sustain the discharge. These forces proportional to the changing magnetic field couple into the plasma volume.

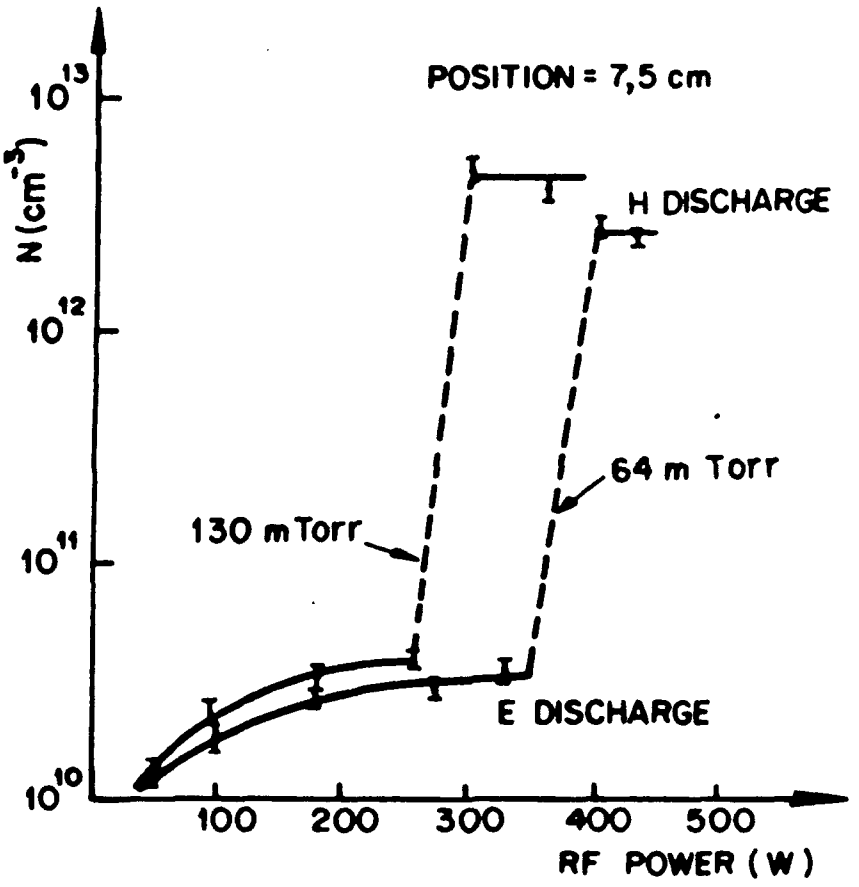

Figure 9. Variation of the plasma density with rf power and the transition from E to H mode of the discharge. (Courtesy of J. Amorim et. al., Jrn. Vac. Sci. Technol. B9, 362 (1991)).

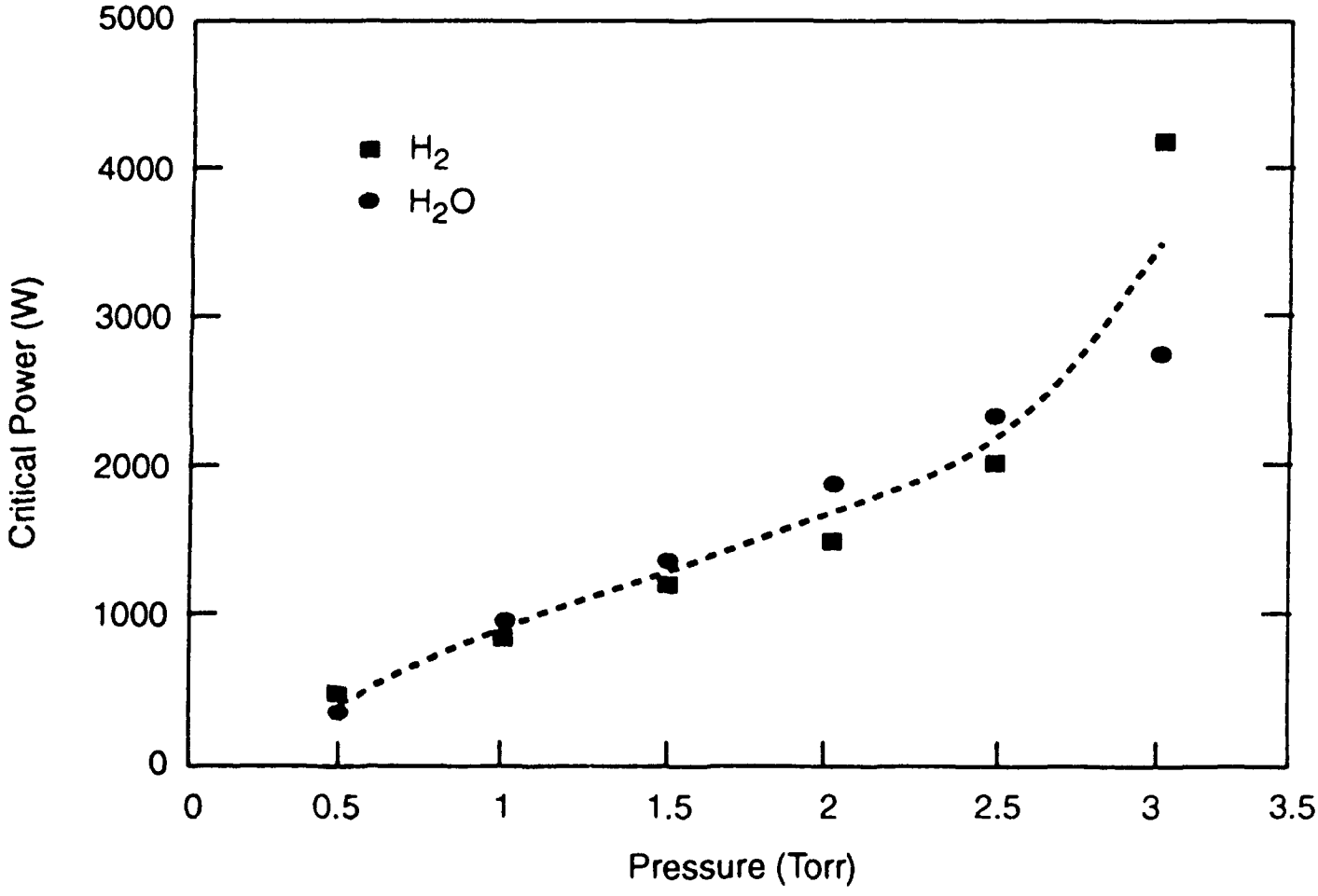

Figure 10. Critical power necessary to initiate a high density induction plasma as a function of pressure for H_2/CH_4 and H_2O/CH_3OH.

4.0 OPTIONS

Having obtained a better understanding of the inherent differences between the capacitive and inductive systems, we began to explore ways to rectify the situation. We see three potential ways by which large area diamond deposition can proceed. All three avenues depend on the generation of large-area high density plasmas.

One approach would be to augment the capacitive plates with permanent magnets arranged such as to produce a high density plasma in the vicinity of the powered cathode. Such an arrangement would be very similar to cathode designs found in magnetron sputtering cathodes. Functionally, we would operate the discharges at pressures higher than sputtering pressures and the use of light gasses such as H_2 and H_2O which would not physically sputter the cathode. Indeed, it may be possible to locate a graphite target on a magnetron sputtering cathodes and obtain chemical vapor transport of carbon from the graphite to the diamond growth surface. Many workers have shown in filament and microwave systems chemical vapor transport diamond growth. We have shown chemical vapor transport in the low pressure rf system using H_2 gas at a pressure of 3 Torr. Kurt J. Lesker loaned a magnetron sputter cathode and power supply to RTI. The sputter cathode and power supply are now at RTI. We have modified a CVD system separate from the Plasma Therm reactor to allow this arrangement to be tested.

A second approach would be to redesign the large area planar capacitive plate so as to make a large area planar inductive plate. It may not be immediately obvious how this can occur. However, some background research into industrial rf induction heating coils shows that large area inductive heating is often accomplished using flat, spiral induction coils. The coil would be shaped similar to the burner on an electric stove. Figure 11 shows schematically the planar inductive design. The coil would create a fairly uniform magnetic field directed radially to the coil. One consequence of the flat spiral design for industrial heating is that unlike the helical coil design flux linkage is lost

on the side of the flat coil opposite the workpiece. For plasma dissociation, we propose to locate the coil inside the plasma gas. The magnetic flux lines, while still emanating from both sides of the flat coil, are encompassed within the plasma gas. At first, the use of an vacuum reentrant rf coil was a fairly difficult idea for us to accept. We believed that current through such a coil would be shorted by the plasma gas. However, work by M. Yamashita in J. Vac. Sci. Technol. A 7, 151 (1989) illustrated quite nicely that a high frequency helical coil reentrant to the vacuum system could produce a high density plasma in a low pressure sputtering application. Figure 12 shows the configuration used by Yamashita. We fabricated and tested a vacuum reentrant helical coil using a matching network similar to that reported by Yamashita et. al. Ongoing work with the reentrant coil has defined a rather specific pressure range 0.100-0.300 Torr wherein a high density water plasma is established for applied powers between 200-500 W. Figure 13 shows optical emission from at water discharge 250 W, inductively coupled, via a vertical reentrant coil. Unlike emission from the capacitively coupled water discharge (see Figure 3), atomic hydrogen emission is quite prevalent. Currently, we are progressing toward a planar reentrant coil. We are confident from our experiences to date that a reentrant planar inductive coil will create a large-area dense plasma suitable for diamond growth. We may be somewhat limited by the maximum power output of the 500 W supply purchased with the Plasma Therm system. The 500 W supply should be capable of producing a large enough high density plasma to permit assessment of growth over the 4" scale targeted in the original proposal.

Lastly, we have recently become aware of a new high frequency microwave plasma source which can be readily scaled to extremely large areas. Increasing the excitation frequency of a plasma, particularly into the GHz range, as an important factor in uniform coupling to large-area chambers. This approach does not rely on electrode arrangements either internal or external, rather the wave is "launched" into the cavity through a window. This has implications for suppression of contaminants, particularly if

combined with "magnetic bottle" arrangements for suppression of chamber wall interactions. According to one company, sources as large as 250 mm with plasma densities of 1E12 cm^3 have been prototyped. Scale of the design to larger areas becomes easier, not more difficult. As part of a silicon processing program at RTI, such a microwave source will be operational at RTI later this calendar year. In addition, Microwave Laboratories, here in the Research Triangle Park, is a major supplier of GHz range traveling wave tubes (TWT) delivering power in the kW range. They are willing to collaborate with us (at no cost) by supplying a TWT unit to interface to the reactor for analysis as a broad area source. They have experience in coupling to chambers as large as 4' x 4' x 4', especially for high frequency sintering of ceramics. The range of available TWT's covers a very broad frequency band stretching out beyond 18 GHz; thus, we can also address the frequency dependence of plasma coupling efficiency and the frequency dependence of the distribution and energetics of excited species.

This is an exciting possibility, particularly in conjunction with the low power chemistries under development at RTI. Microwave laboratories is eligible for SBIR work and has worked on one or more SBIR programs.

We do not currently know which of these approaches will offer the best approach to scaling diamond growth technology to large areas with accompanying high density plasmas. We are confident that the application of these high density sources will produce diamond at reasonable rates so as to be economically competitive.

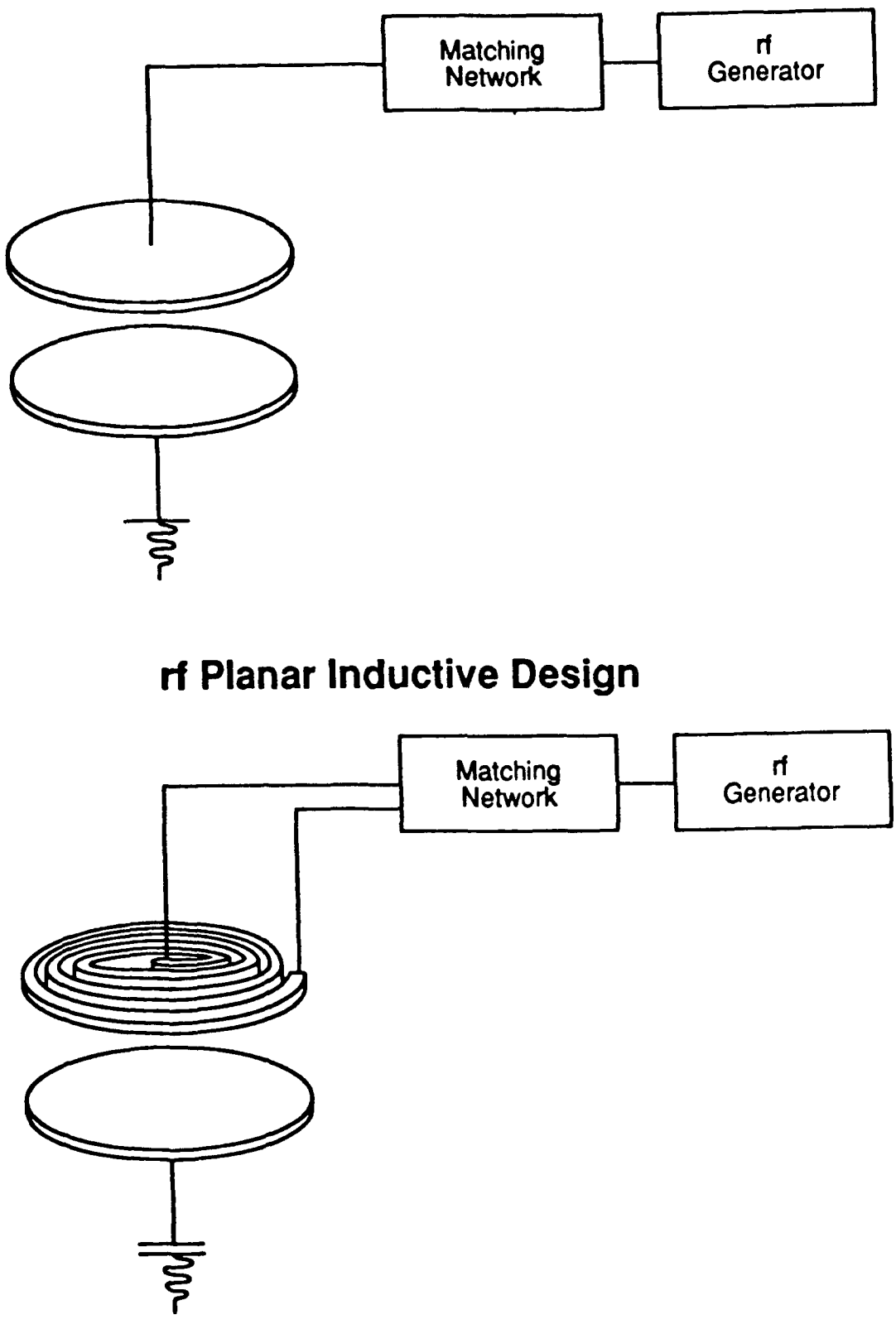

Figure 11. Planar capacitive design vs. planar inductive design.

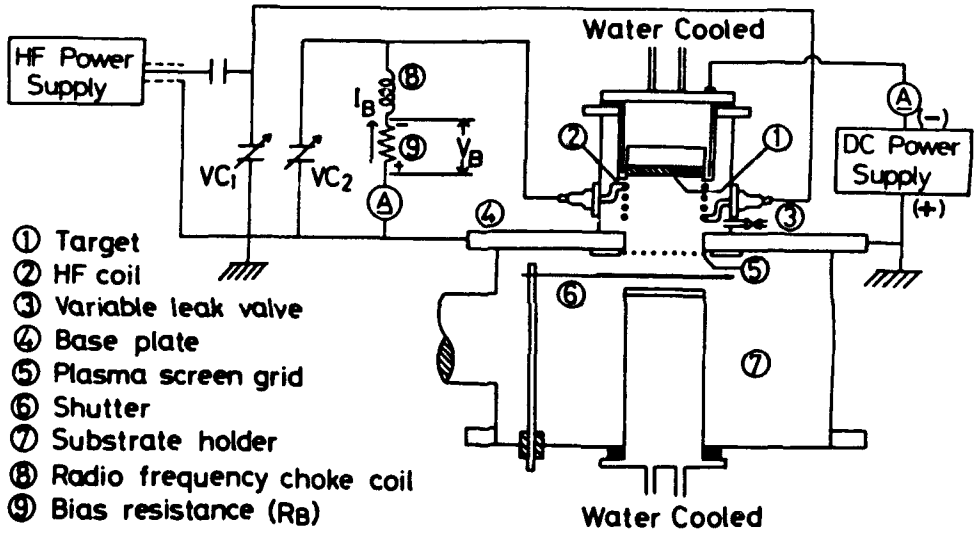

Figure 12. Reentrant coil design of Yamashita (J. Vac. Sci. Technol. A7, 151 (1989)).

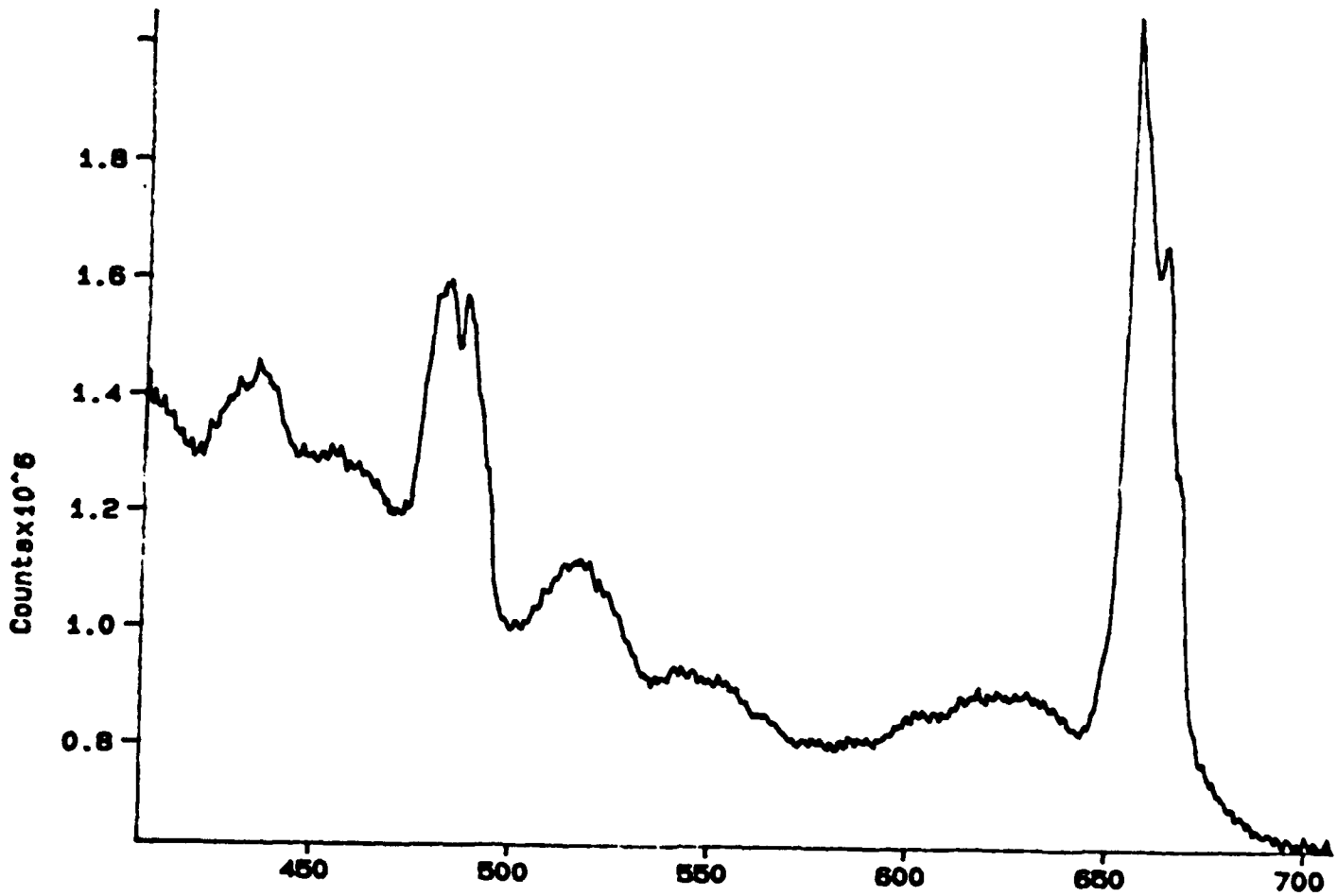

Figure 13. Optical emission from 0.250 Torr water discharge inductively coupled using a reentrant helical coil.

5.0 PROGRAM STATUS

We are about one-half the way through the one year program. We have expeditiously assessed the rf capacitively coupled systems and have determined some fundamental differences in the plasma coupling which probably accounts for the failure of the rf capacitive system to produce diamond as readily as rf inductive systems have. Given, in-house rf-capacitive and rf-inductive equipment, we were in an unique position to provide a critical assessment of the chemical differences in those discharges. We have determined that the inductive discharges and for more dissociative than the capacitive discharges. We are modifying the large area capacitive system to study large area planar inductive designs. Such coils would merely replace the standard powered cathode in the capacitive design with a powered planar inductor. Since no information appears available in the plasma literature concerning planar inductive designs, we are pursuing the development of a reentrant planar inductive design by first establishing a high density plasma with a reentrant helical inductive design. We have accomplished production of a high density water plasma with a reentrant 50 mm diam helical coil. Work is proceeding by gradually "flattening" the helical coil to provide a large area high density plasma.

Given that a technical limitation of the current rf power supply does not thwart progress, the program appears to be well on its way to demonstrating large area diamond growth with a re-entrant, planar rf coil design.

6.0 APPENDIX

Formation of Diamond Films From Low Pressure rf Induction Discharges

R.A. Rudder, G.C. Hudson, R.C. Hendry, R.E. Thomas, J.B. Posthill,
and R.J. Markunas

Research Triangle Institute, Research Triangle Park, NC 27709-2194

Summary

Diamond films have been deposited in a low pressure, rf induction plasma assisted chemical vapor deposition system. The rf induction system confines the plasma at the low pressures of operation 0.010 - 10.00 Torr so as to permit efficient dissociation of the reactant gasses. A variety of chemical systems have been used to deposit diamond. The chemical systems have included traditional H_2/CH_4 discharges containing 0.5 - 2.0% CH_4, have included H_2/CF_4 discharges containing 4 - 16% CF_4, and have included water vapor discharges containing high concentrations of alcohol and/or acetic-acid vapors. No molecular hydrogen is admitted to the growth chamber for the water-based processes. The water vapor becomes the functional equivalent of the molecular hydrogen process gas used in more traditional H_2/CH_4 discharges. The success of the low pressure rf induction plasma for diamond growth from the wide variety of chemical systems is predicated on the generation of a high electron density plasma. Parent gaseous molecules are converted into appropriate high temperature stable products such as H, H_2, CO, and C_2H_2 as they traverse the plasma. Quadrupole mass spectroscopy has been used to study the conversion of the water-alcohol vapors to H_2, CO, and C_2H_2 as they pass through the rf plasma. 99% of the CH_3OH is converted into H_2, H_20, and C_2H_2 products. These studies show plasma conversion of H_2O into molecular H_2. The excess oxygen is rapidly consumed into CO through interactions of the O, presumably with solid carbon sources. Optical emission from both the water-based discharges and the molecular hydrogen based discharges shows the propensity for atomic hydrogen generation from these low pressure rf-induction discharges.

INTRODUCTION

Diamond film production via chemical vapor deposition has clearly been demonstrated by a vast number of chemcial vapor deposition (CVD) techniques. [1-10] Typically, the ability to produce diamond via those CVD techniques depends critically on the production of atomic hydrogen whether that was through interaction of molecular hydrogen with hot-filaments, microwave plasmas, dc arc discharges, or atmospheric rf plasma jets. Alternatively, oxy-acetylene torches have been used for the growth of diamond wherein the hot chemical flame provides atomization of gasses present in the flame.[6,7] We previously reported on the use of a low pressure (less than 10 Torr) rf induction plasma technique for the growth of diamond films from many different feed stock gasses ranging from traditional H_2/CH_4 discharges,[11-15] to halogenated H_2/CF_4 discharges, [16,17] to H_2O/alcohol discharges, [18] and to H_2O/alcohol/acetic-acid discharges.[19] The capability for diamond growth from these varied systems can be associated with the efficient production of atomic hydrogen in the low pressure, rf induction discharges.

This paper reviews briefly conditions upon which diamond growth proceeds from the various gas mixtures and then concentrates on analysis and characterization of the water-methanol system for diamond growth. This system is the simplest of the water-based systems and yields great insight into the plasma chemistry. The water-based system may also be of greatest interest to those concerned with commercialization of diamond films. As compared to more traditional growth processes involving H_2/CH_4, the water-based processes offer numerous advantages. Those advantages include:

- low temperature growth,
- low pressure operation,
- the availability of large rf power supplies,
- the elimination of explosive gasses from the growth process.
- the elimination of compressed gasses from the growth process

EXPERIMENTAL EQUIPMENT AND PROCEDURES

A description of the chemical vapor deposition system used in this work has been previously reported. [11-13] A schematic of the system is shown in Figure 1. The system consists of a 50 mm id plasma tube appended to a standard six-way cross. The plasma tube contains an integral water jacket to dissipate heat from the interior quartz wall. A radio frequency (13.56 MHz) induction coil couples power from the rf power supply into the plasma discharge. Samples are located on a graphite carrier located immediately underneath the induction coil. Samples are heated indirectly by induction current heating in the graphite susceptor. If higher temperatures are desired, a supplemental resistive graphite heater can be used to increase the temperature of the graphite susceptor. Care is taken not to insert the graphite carrier into the plasma coil. Insertion into the coil would result in much greater heating of the graphite susceptor.

Gasses from compressed sources are introduced into the plasma system through a gas feed at the top of the plasma tube. The ratio of one gas to another is controlled by adjusting the relative mass flow rates of each component into the plasma system. Gasses above liquid reservoirs (water, alcohol, acetic-acid) are introduced into the chamber through a leak valve on a storage tank which contains solutions of the water/alcohol or water/acetic-acid/alcohol. Gasses from the liquid reservoirs have been introduced either from the top of the plasma tube or at the base of the plasma tube. Either place of introduction can result in diamond growth for an appropriate water to alcohol ratio. In this work, the water to alcohol ratio has been controlled by the relative volumetric ratio in the gas phase and the respective vapor pressure of each component. The practice of mixing the solutions into one storage tank allows a convenient method for evaluating different ratios of water-to-alcohol without the necessity of a gas manifold. There will be some depletion from the solution of the higher vapor pressure component.

Samples are introduced to the growth system through a vacuum load lock. Prior to insertion, samples have been subjected to a diamond abrasive treatment with 1 μm diamond paste to enhance nucleation. Diamond growth proceeds by initiating a rf induction plasma with sufficient power to create intense atomic hydrogen emission. For each gas combination and pressure, there exists a critical power at which the discharge suddenly becomes locally very intense within the rf coils. The authors believe that this power threshold is a consequence of the power coupling changing from E-field coupling at low powers to B-field coupling at high powers. J. Amorim et al. [20] have shown in low pressure Ar plasmas that the coupling changes from capacitive coupling to induction coupling at a critical power level depending on the Ar pressure. For Ar at 130 mTorr, the critical power is ~275 W. The B-field coupling is characterized by intense plasma luminosity from a region of high electron density, $\sim 10^{12}$ cm^{-3}. The E-field coupling at lower powers is characterized by weak plasma luninosity from a region of low electron density, $\sim 10^{10}$ cm^{-3}. Establishing the high electron density plasma is critical in order to produce diamond growth in this low pressure rf induction system. Attempts to deposit diamond under low density plasma conditions with concentrations of CH_4 in H_2 used for diamond deposition under high power conditions have resulted in no film growth.

This work concentrates on understanding the necessity of the high electron density plasma for diamond growth by examining the plasma chemistry through optical emission and quadrupole mass spectroscopy. Optical emission spectroscopy has determined the proficiency of the various process to produce atomic hydrogen. Quadrupole mass spectroscopy (performed through differential sampling of the gasses at the base of the reactor tube) has determined reaction products formed as the parent gasses traverse the high-temperature plasma region. Following diamond deposition, samples have been analyzed using scanning electron microscopy (SEM) and Raman spectroscopy to ascertain the quality of diamond growth.

EXPERIMENTAL RESULTS AND DISCUSSION

Previous work [11-19] has demonstrated the diversity of the low pressure rf plasma technique for the growth of diamond films from a variety of chemical systems under vastly different input powers, substrate temperatures, and pressure conditions. Figure 2 depicts diamond growth from three different chemical systems (H_2:CH_4, H_2O:CH_3OH, and H_2O:CH_3COOH:CH_3OH). Table I shows experimental differences between the conditions used to deposit diamond in Figures 2a-c. Despite the vast differences in deposition conditions, well faceted diamond growth occurs under all these conditions even at low temperatures and low input power. In addition, the low temperature growth capability now permits diamond growth studies on relatively low-melting-temperature materials such as Al.

Critical to the diamond growth in all these processes is the establishment of a high density plasma. While the amount of power necessary to achieve a high density varies from one gas mixture to another, in general, lower pressure discharges require less power to achieve induction coupling. Figure 3 is a plot of the critical power necessary to achieve a high density plasma for the H_2:CH_4 and H_2O:CH_3OH systems as a function of pressure. The threshold power necessary to establish the high density plasma varies almost linearly with pressure (in this pressure range) for the H_2O:CH_3OH system. The H_2:CH_4 system behaves supralinearly so that at higher pressures there is a significant power difference between operating a water-based process verses a molecular-hydrogen-based process.

Optical Emission

Optical emission spectroscopy has been used to confirm atomic hydrogen generation from these low pressure discharges. Figure 4 shows the optical emission from a 3 Torr 1% CH_4 in H_2 discharge. The emission is dominated by the 656 nm atomic H emission due to an optical transition from the n=3 to the n=2 energy level. Correspondingly, the discharge has a

characteristic red color. High plasma density water discharges, also show a characteristic red color with emission dominated by the 656 nm atomic H emission. Addition of CH_3OH to the high density water discharges results in a bluish-red emission still with dominate atomic H emission. Figure 5 shows an optical emission spectrum from a 1 Torr H_2O:CH_3O discharge containing approximately equal parts H_2O and CH_3OH in the gas phase. Like the diamond producing 1% CH_4 in H_2 discharge, emissions from the water-methanol show intense atomic hydrogen emission even with high CH_3OH concentrations. In contrast, low plasma density water discharges are bluish in color with the dominant emission from OH bands and very little atomic H emission.

Quadrupole Mass Spectroscopy

Quadrupole mass spectroscopy has been used to monitor the conversion of parent H_2O, CH_3OH molecules to high-temperature-stable products as they traverse the plasma. Figure 6 shows H_2O^+ and CH_3O^+ ion counts before and after initiation of the high density plasma. Figure 6 also shows those ion counts as a function of the volumetric concentration of methanol in the liquid reservoir. Before initiation of the plasma, the ratio of H_2O^+ and CH_3O^+ ion counts reflect Raoult's Law relating the partial pressures above a composite solution to the vapor pressure of the constituent times the mole fraction of the constituent in solution. However, after plasma initiation, a rather dramatic occurrence is observed. Nearly all the CH_3OH is converted upon traversing the plasma. The CH_3O^+ counts after plasma initiation are only a couple percent of the original CH_3O^+ counts. Even more knowledge of the plasma dissociation is obtained when one examines by-products from the H_2O:CH_3OH plasma discharge. Figure 7 shows the dominant conversion products observed as a function of methanol concentration in the reservoir. A high atomic fraction of molecular H_2 is produced in the gas phase almost regardless of the CH_3OH concentration. Molecular H_2 is the dominant species produced by the H_2O:CH_3OH plasma discharge. CO and C_2H_2 are also produced as a by-product of the H_2O:CH_3OH plasma discharge. At high water concentrations (i.e. high O fraction), CO is the preferred gaseous carbon product. At high CH_3OH concentrations (i.e. low O fraction), C_2H_2 is the preferred

gaseous carbon product. Thus, we have identified H_2, CO, and C_2H_2 as conversion products in the high density water-methanol plasma discharges. The water concentrations in the discharge remain high, but the CH_3OH concentrations are reduced to only a small percentage of their original concentrations. The production of CO and C_2H_2 can occur via direct conversion of CH_3OH into CO or C_2H_2 or via gasification of solid carbon through interactions of O and H with graphite.

It is abundantly clear that the water-based processes convert parent H_2O and CH_3OH molecules into more stable high temperature products. One might estimate an effective temperature of the plasma by comparing the H_2O to H_2 conversion in the plasma to that predicted from thermodynamic equilibrium theory at high temperatures. Lede et. al. have reported on the direct thermal decomposition of water at elevated temperatures (1500-4000 K) at pressures from 10^4 to 10^6 Pa. [21] At temperatures in excess of 3300 K, H_2O is no longer the dominant species. Atomic H and atomic O are the dominant species at high temperature. From the quadrupole data in Figure 7, one can estimate the partial pressure of H_2O in the system with the discharge initiated. By taking into account differences in ionization efficiency and differences in mass conductances of H_2, H_2O, and CO, we estimated the partial pressure of H_2O in the growth chamber with the discharge on to be 0.28 Torr. Compared to the partial pressure of 1 Torr for H_2O in the system before the discharge was initiated, the amount of H_2O dissociated by the plasma is 72%. Referring to the 10^4 Pa data given by Lede et. al. [21], dissociation of 72% of the water would require a temperature of ~ 3100 K for homogeneous dissociation. Thus, the low pressure rf induction technique generates an extremely hot plasma. For comparison at 2300K, only 4% of the water is decomposed under atmospheric pressure. (This amount is expected to increase some as the pressure is reduced). One key to the success of the growth of diamond at low pressures is undoubtedly the high generation rate of atomic hydrogen in these rf induction discharges. At low pressures, atomic H can rapidly diffuse from the plasma discharge and recombine on reactor walls. The diffusion depletes the gas phase of atomic H. Correspondingly, high generation rates must occur to maintain a high concentration of atomic hydrogen. The high

generation rates are insured by the high temperatures of the rf induction plasma.

CONCLUSIONS

Diamond films have been produced from a great variety of chemical systems in a low pressure rf-induction plasma-assisted CVD system. Key to this process is the generation of high density plasmas in which efficient atomic hydrogen is possible. Optical emissions from both the water-methanol and the H_2/CH_4 high density discharges show strong atomic H emission. Quadrupole mass spectroscopy shows that the H_2O:CH_3OH system is converted into high temperature stable products H_2, CO, and C_2H_2 Substantial concentrations (~ 25%) of water remain in the system, but almost all the CH_3OH is converted. The production of CO and C_2H_2 can occur via direct conversion of CH_3OH into CO or C_2H_2 or via gasification of solid carbon interactions of O and H with nearby graphite. The ability to sustain a high plasma density discharge at low input powers allows diamond growth from the H_2O:CH_3OH system to proceed at reduced pressures where recombination on the reactor walls can deplete atomic H from the gas phase. Estimates of an effective plasma temperature based on the degree of H_2O dissociation shows the effective temperature to be ~ 3100 K. Such temperatures are sufficient for atomic hydrogen generation in these low pressure rf induction discharges.

Acknowledgments:

The authors wish to thank the support of this work through the SDIO/IST organization and DARPA via ONR contracts N-00014-86-C-0460 and N-000014-91-C-0177. The authors wish to thank Dr. T.P. Humphreys and Dr. R.J. Nemanich for Raman support during this work. The authors wish to thank D.P. Malta, S. Ammons, and R.V. Durkee for outstanding technical support of this work at Research Triangle Institute.

Table I

Sample	Figure	Pressure	rf Power	Substrate	T_s	Gas	Mixture
#1	2a	5.0 Torr	2000 W	Si	800 °C	H_2:CH_4	99:1
#2	2b	1.0 Torr	1000 W	Fused Silica	300 °C	H_2O:CH_4O	2:1 ϒ
#3	2c	0.5 Torr	800 W	Al	300 °C	H_2O:$C_2H_4O_2$:CH_4O	2:2:1 ϒ

ϒ These are the volumetric ratios of the constituents in solution.

REFERENCES

1. B. Derjaguin and V. Fedoseev, Russ. Chem. Rev. 39, 783 (1970).

2. B.V. Spitsyn, L.L. Bouilov, and B.V. Derjaguin, J. Cryst. Growth 52, 219 (1981).

3. S. Matsumoto, Y. Sato, M. Kamo, and N. Setaka, Jpn. J. Appl. Phys. 21, 183 (1982).

4. Y. Hirose and Y. Teresawa, Jpn. J. Appl. Phys. 25, L51 (1986).

5. M. Kamo, Y. Sato, S. Matsumoto, and N. Setaka, J. Cryst. Growth 62, 642 (1983).

6. L.M. Hanssen, W.A. Carrington, J.E. Butler, and K.A. Snail, Mater. Letters 7, 289 (1988).

7. G. Janssen, W.J.P. Van Enckevort, J.J.D. Schaminee, W. Vollenberg, L.J. Giling, M. Seal, J. Cryst. Growth 104, 752 (1990).

8. Peter K. Bachmann, Dieter Leers, and Hans Lydtin, Diamond and Related Materials 1, 1 (1991).

9. M. Buck, T.J. Chuang, J.H. Kaufman, and H. Seki, Mat. Res. Soc. Symp. Proc. 162, 97 (1990).

10. C.F. Chen, T. M. Hon and C.L. Lin, presented at 18th Int. Conf. on Metallurgical Coatings and Thin Films (ICMCTF), San Diego, CA, April 23, 1991.

11. R.A. Rudder, G.C. Hudson, Y.M. LeGrice, M.J. Mantini, J.B. Posthill, R.J. Nemanich, and R.J. Markunas, MRS Extended Abstracts EA19, 89 (1989).

12. R.A. Rudder, G.C. Hudson, R.C. Hendry, R.E. Thomas, J.B. Posthill, and R.J. Markunas, "Applications of Diamond Films and Related Materials", Materials Science Monograph 73, 583 (1991).

13. R.A. Rudder, G.C. Hudson, J.B. Posthill, R.E. Thomas, R.J. Markunas, R.J. Nemanich, Y.M. LeGrice, T.P. Humphreys, Acetylene Production in a Diamond-Producing Low Pressure rf-Plasma-Assisted Chemical Vapor Deposition Environment, Second International Symposium on Diamond Materials (held during the 179th Meeting of the Electrochemical Society), 1991, in press.

14. J.B. Posthill, R.A. Rudder, G.C. Hudson, D.P. Malta, R.E. Thomas, R.J. Markunas, T.P. Humphreys, R.J. Nemanich, D. Black, Substrate Effects and the Growth of Homoepitaxial Diamond(100) Layers Using Low Pressure rf-Plasma-Enhanced Chemical Vapor Deposition, Second International Symposium on Diamond Materials (held during the 179th Meeting of the Electrochemical Society), 1991, in press.

15. R.A. Rudder, J.B. Posthill, G.C. Hudson, D. Malta, R.E. Thomas, and R.J. Markunas, New Diamond Science and Technology, 1991 MRS Int. Conf. Proc., p. 425-430.

16. R.A. Rudder, G.C. Hudson, J.B. Posthill, R.E. Thomas, and R.J. Markunas, Appl. Phys. Lett. 59, 791 (1991).

17. R.A. Rudder, G.C. Hudson, R.C. Hendry, R.E. Thomas, J.B. Posthill, and R.J. Markunas, "Applications of Diamond Films and Related Materials", Materials Science Monograph 73, 395 (1991).

18. R.A. Rudder, G.C. Hudson, J.B. Posthill, R.E. Thomas, R.C. Hendry, D.P. Malta, R.J. Markunas, T.P. Humphreys, and R.J. Nemanich, Appl. Phys. Lett. 60, 329 (1992).

19. R.A. Rudder, J.B. Posthill, G.C. Hudson, D.P. Malta, R.E. Thomas, R.J. Markunas, T.P. Humphreys, and R.J. Nemanich, to appear in conference proceedings on Wide-Band Gap Semiconductors, Fall MRS 1992, Boston.

20. J. Amorim, H.S. Maciel, and J.P. Sudano, J. Vac. Sci, Technol. B9, 362 (1991).

21. J. Lede, F. Lapicque, J. Villermaux, B. Cales, A. Ounalli, J.F. Baumard, and A.M. Anthony, Int. J. Hydrogen Energy 7, 939 (1982).

LIST OF FIGURES

Figure 1

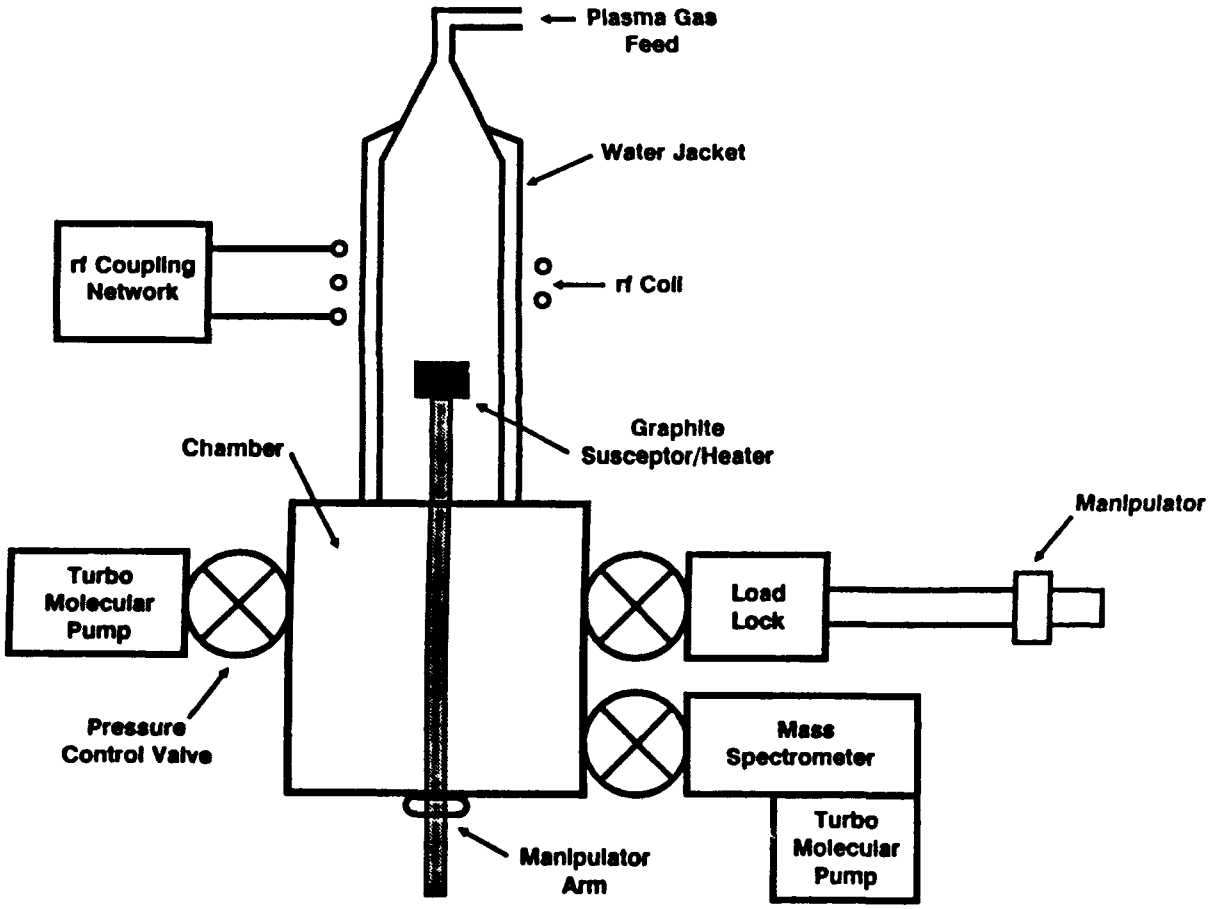
Plasma Gas Feed
Water Jacket
rf Coupling Network
rf Coil
Graphite Susceptor/Heater
Chamber
Manipulator
Turbo Molecular Pump
Load Lock
Pressure Control Valve
Mass Spectrometer
Turbo Molecular Pump
Manipulator Arm

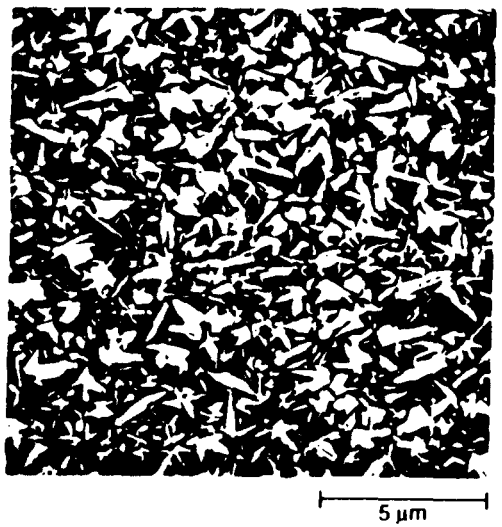

(2a)

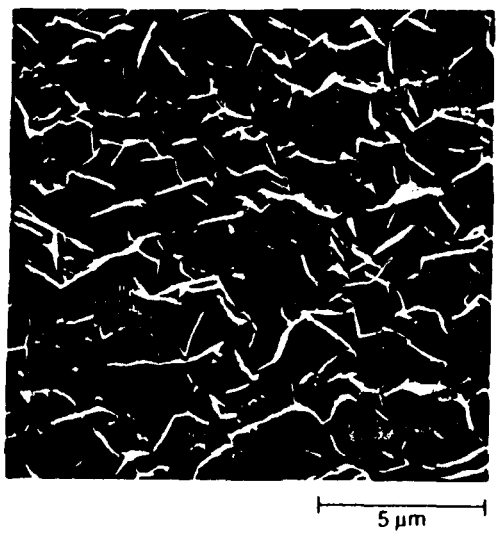

(2b)

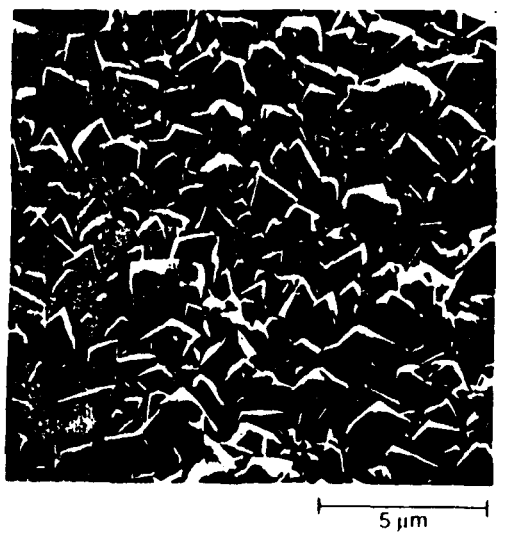

(2c)

Figure 3

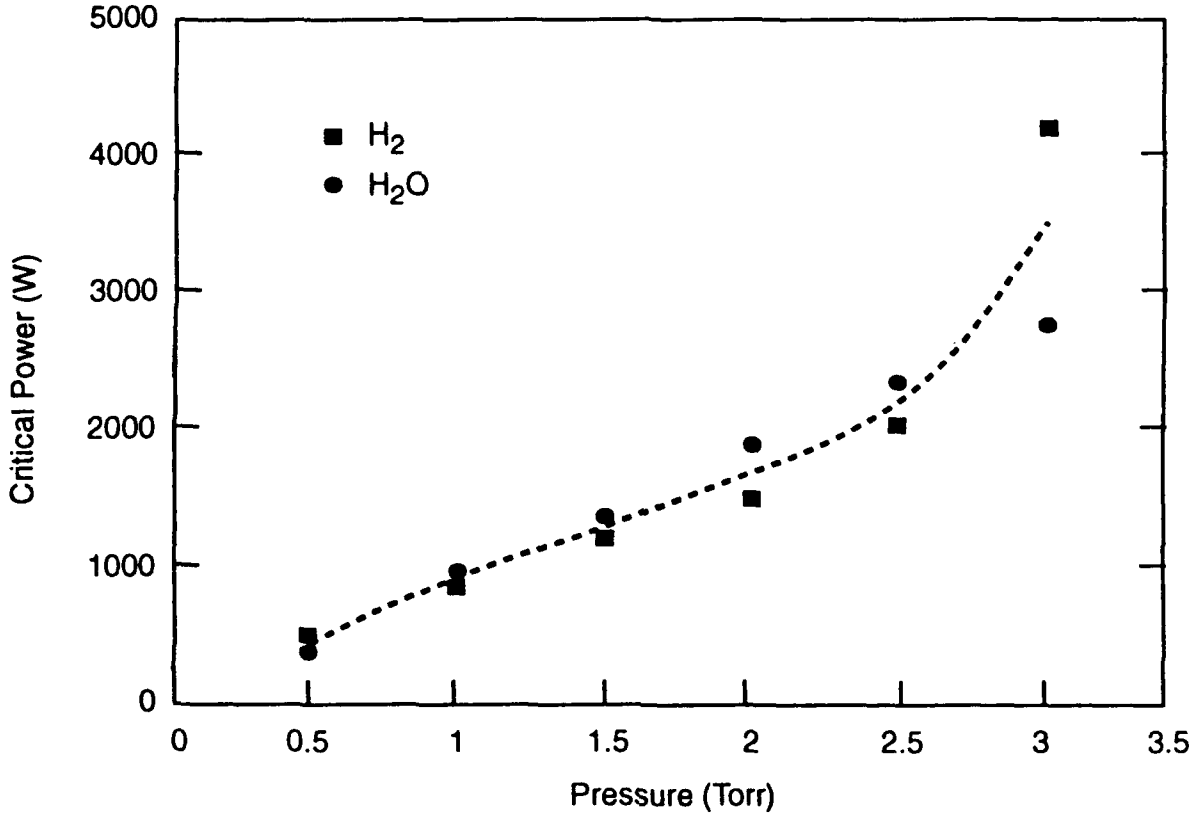
5000
4000
3000
2000
1000
0
Critical Power (W)
H_2
H_2O
0
0.5
1
1.5
2
2.5
3
3.5
Pressure (Torr)

Figure 4

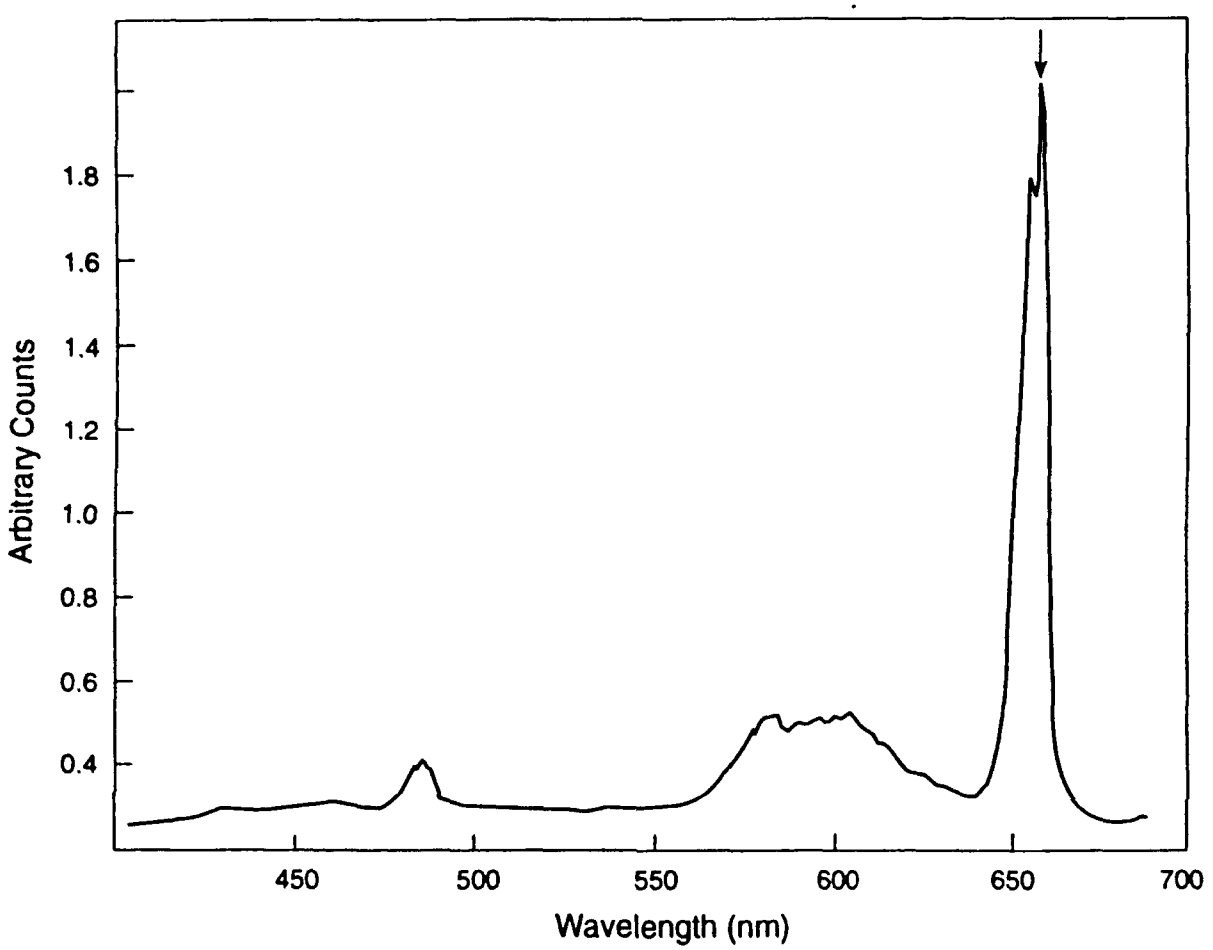
Arbitrary Counts
1.8
1.6
1.4
1.2
1.0
0.8
0.6
0.4
450
500
550
600
650
700
Wavelength (nm)

Figure 5

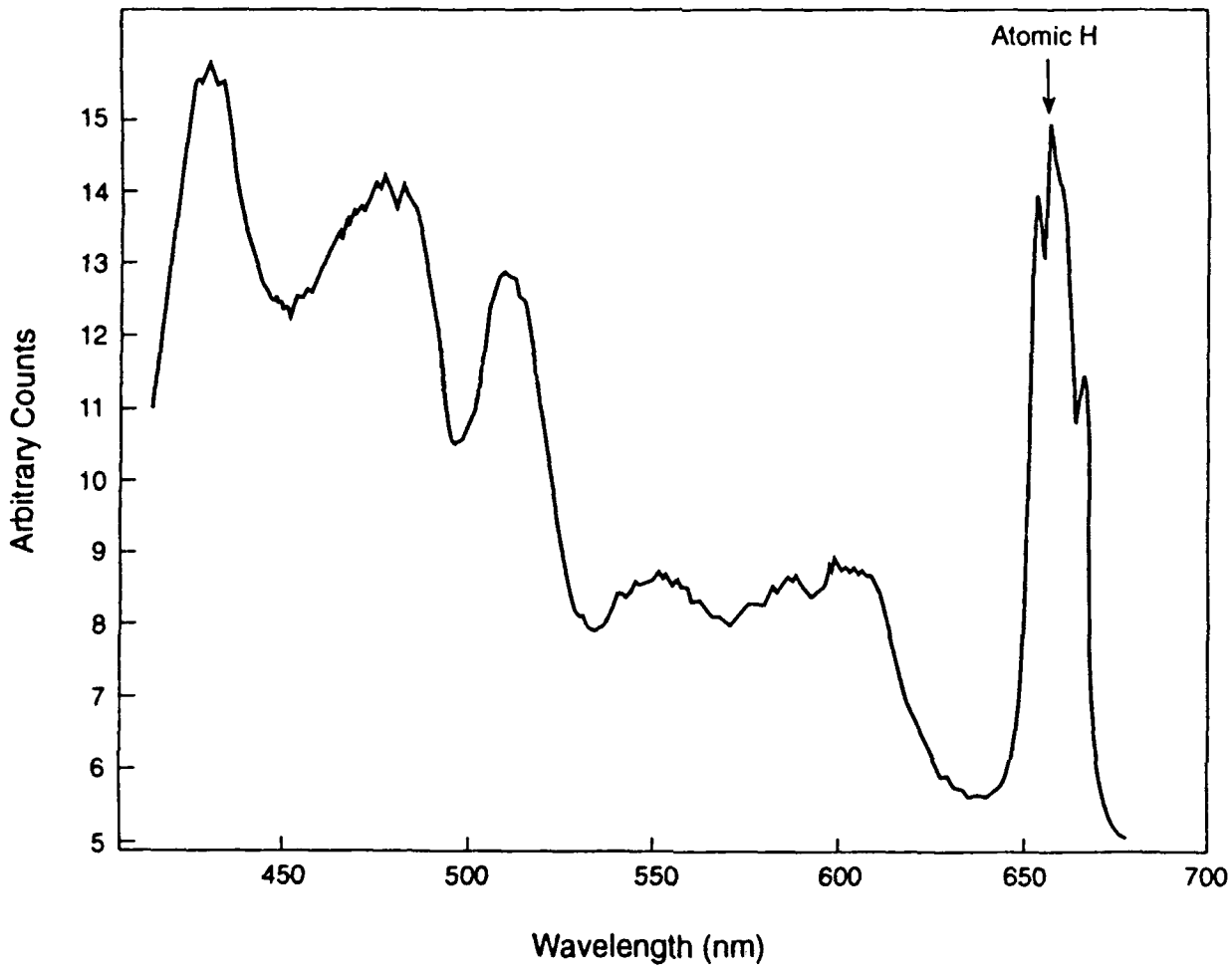
Atomic H
Arbitrary Counts
15
14
13
12
11
10
9
8
7
6
5
450
500
550
600
650
700
Wavelength (nm)

Figure 6

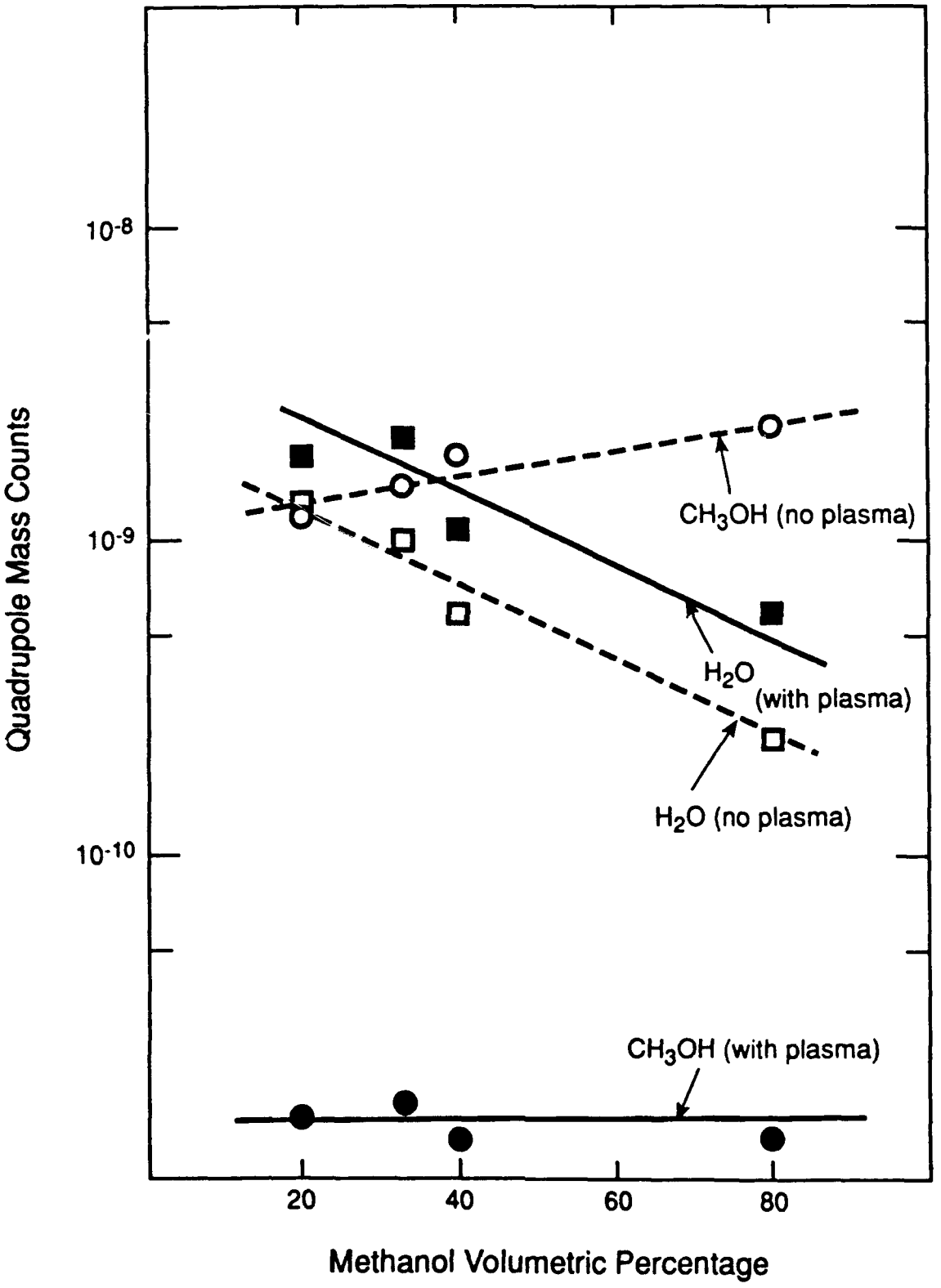
Quadrupole Mass Counts
10-8
10-9
10-10
CH3OH (no plasma)
H2O
(with plasma)
H2O (no plasma)
CH3OH (with plasma)
20
40
60
80
Methanol Volumetric Percentage

Figure 7

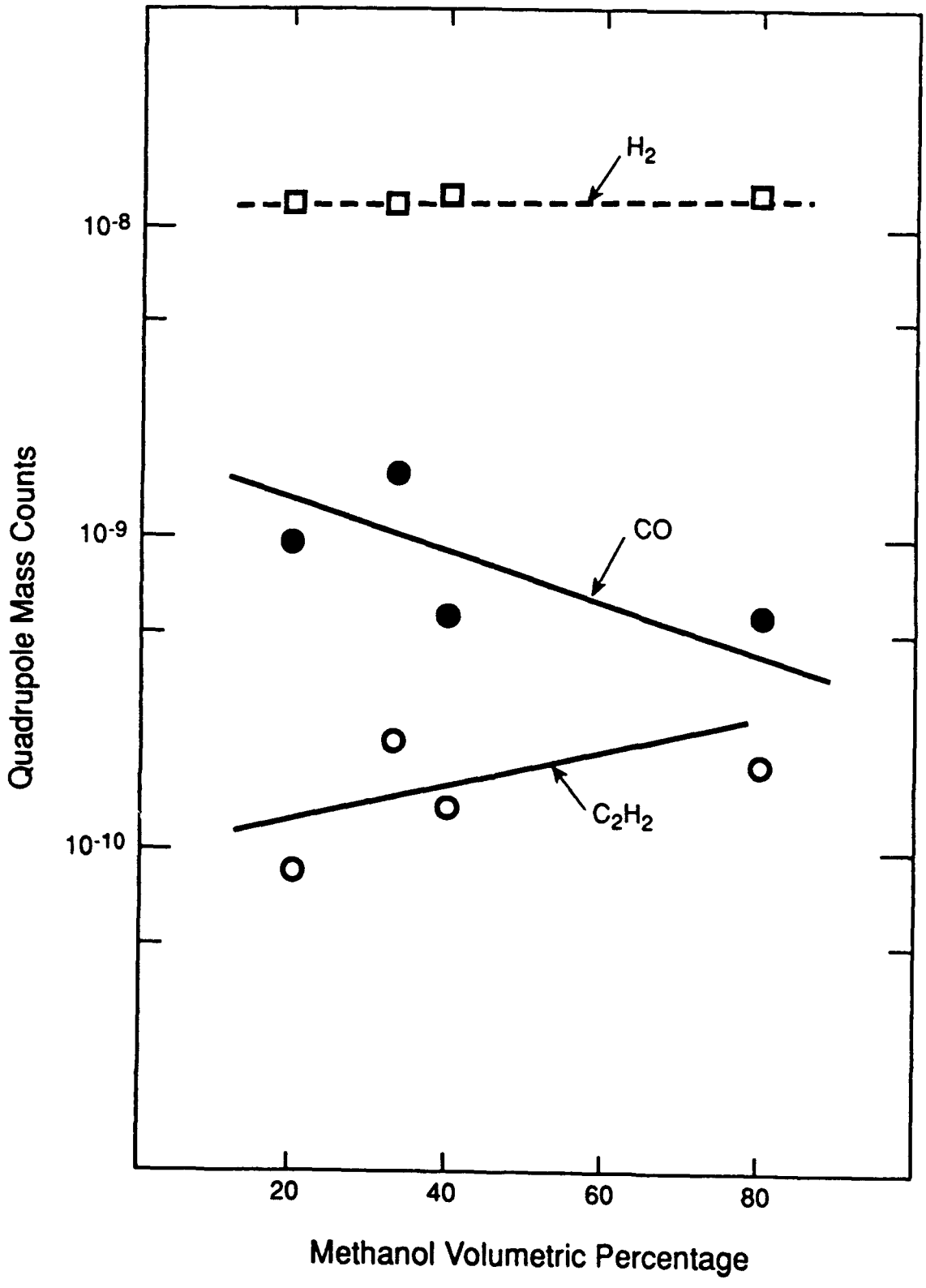
H2
CO
C2H2
10-8
10-9
10-10
Quadrupole Mass Counts
20
40
60
80
Methanol Volumetric Percentage